

SUPPLEMENTARY INFORMATION

GREGOR: Evaluating global enrichment of trait-associated variants in epigenomic features using a systematic, data-driven approach

Ellen M Schmidt¹

Email: schellen@umich.edu

Ji Zhang²

Email: zhangji@med.umich.edu

Wei Zhou¹

Email: zhwei@med.umich.edu

Jin Chen²

Email: jich@umich.edu

Karen L Mohlke³

Email: mohlke@med.unc.edu

Y Eugene Chen²

Email: echenum@med.umich.edu

Cristen J Willer^{1,2*}

Email: cristen@umich.edu

1. Department of Computational Medicine and Bioinformatics, University of Michigan, Ann Arbor, MI 48109, USA

2. Department of Internal Medicine, Division of Cardiovascular Medicine, University of Michigan, Ann Arbor, MI 48109, USA

3. Department of Genetics, University of North Carolina, Chapel Hill, NC 27599, USA

* Corresponding Author:

Division of Cardiovascular Medicine and Department of Human Genetics

University of Michigan Medical School

5804 Medical Science II

1241 E. Catherine St.

Ann Arbor, MI 48109-5618

734-647-6018

Table of Contents

| | |
|---|---|
| SUPPLEMENTARY METHODS | 3 |
| SUPPLEMENTARY FIGURES | 6 |
| Supplementary Figure 1. Summary of GREGOR variant enrichment method | 6 |

| | |
|--|----|
| Supplementary Figure 2. Enrichment of lipid-associated variation in DNase hypersensitive sites using different parameter values | 7 |
| Supplementary Figure 3. Enrichment <i>P</i> -values estimated using 10,000 permutations (y-axis) and the sum of binomial trials as implemented in GREGOR (x-axis) | 8 |
| Supplementary Figure 4. QQ plots of enrichment performance for lipid-associated variation in DNase hypersensitive sites and control sets | 9 |
| Supplementary Figure 5. Fold enrichment (A) and enrichment <i>P</i> -values (B) for lipid-associated variation in DNase hypersensitive sites (DHSs) of different tissues and at different ‘consensus thresholds’ | 10 |
| Supplementary Figure 6. Matrix of fold enrichment for five sets of trait-associated variants in predicted chromatin states in nine human cell types | 12 |
| Supplementary Figure 7. Prioritization of lipid-associated loci for functional follow-up | 15 |
| Supplementary Figure 8. Physical overlap of variants at six lipid loci (SNPs within $r^2 > 0.7$ of the GWAS index SNP) with ChIP-seq or DNase-seq binding sites for lipid-related ENCODE features (..... | 15 |
| A. <i>SORT1</i> (sortilin 1) | 16 |
| B. <i>FAM117B</i> (family with sequence similarity 117, member B) | 17 |
| C. <i>ANGPTL8</i> (Angiopoietin-like protein 8; C19orf80: chromosome 19 open reading frame 80).... | 18 |
| D. <i>SPTLC3</i> (serine palmitoyltransferase, long chain base subunit 3) | 19 |
| E. <i>ADH5</i> (alcohol dehydrogenase 5 (class III), chi polypeptide)..... | 20 |
| F. <i>IRF2BP2</i> (interferon regulatory factor 2 binding protein 2)..... | 21 |
| SUPPLEMENTARY TABLES | 22 |
| Supplementary Table 1. ENCODE DNase hypersensitivity sites from various tissues are categorized into broader tissue groups for enrichment analysis..... | 22 |
| Supplementary Table 2. Enrichment of GWAS loci in DNase hypersensitive sites of common tissues. | 35 |
| A. Body Mass Index (BMI) and Blood Pressure (BP)..... | 35 |
| B. Coronary Artery Disease (CAD), Lipids, and Type 2 Diabetes (T2D)..... | 36 |
| Supplementary Table 3. Fold enrichment of lipid loci in DNase hypersensitive sites at different consensus thresholds..... | 38 |
| Supplementary Table 4. Enrichment of GWAS loci for five traits or diseases (BMI; Body Mass Index, BP; Blood Pressure, CAD; Coronary Artery Disease, Lipids, T2D; Type 2 Diabetes) in predicted chromatin states | 40 |
| Supplementary Table 5. Enrichment of lipid loci in transcription factor binding sites and histone modifications from relevant Tier 1 and Tier 2 cell types. | 48 |
| Supplementary Table 6: Primers used in luciferase expression constructs. | 53 |

| | |
|-------------------------------|----|
| SUPPLEMENTARY REFERENCES..... | 55 |
|-------------------------------|----|

SUPPLEMENTARY METHODS

Data acquisition and pre-processing

DNase-seq ENCODE data for all available cell types were downloaded in the processed “narrowPeak” format. The local maxima of the tag density in broad, variable-sized “hotspot” regions of chromatin accessibility were thresholded at FDR 1% with peaks set to a fixed width of 150bp. Individual cell types were further grouped into 41 broad tissue categories (<http://genome.ucsc.edu/ENCODE/cellTypes.html>) by taking the union of DHSs for all related cell types and replicates (**Table S1**). We also obtained a set of BED files in hg19 assembly from the Integrative Analysis and original ENCODE analysis. These data include uniformly processed datasets in 125 cell types generated by the “Open Chromatin” (Duke University) and University of Washington (UW) ENCODE groups. Data processed during the ENCODE Integrative Analysis were downloaded for available tissues. Otherwise, data from the original ENCODE analysis were obtained. We examined the overlap of DHSs across different cell types, and found that as expected, cell types derived from related tissues generally clustered together. In addition, we examined chromatin state segmentation by HMM generated from ENCODE/Broad in nine human cell types, as well as transcription factor binding sites by ChIP-seq from the ENCODE Analysis Working Group (AWG) including ENCODE/HudsonAlpha (HAIB), ENCODE/Stanford/Yale/Davis/Harvard (SYDH), ENCODE/University of Chicago, ENCODE/Open Chrom (UT Austin), and ENCODE/University of Washington (UW). No datasets analyzed were under embargo.

Selecting matched control SNPs for GWAS index SNPs

For each GWAS locus, we selected a set of matched control SNPs based on 3 criteria: 1) number of variants in LD ($r^2 > 0.7$; ± 8 variants), 2) minor allele frequency ($\pm 1\%$), and 3) distance to nearest gene ($\pm 11,655$ bp). To calculate the distance to the nearest gene, we calculated the distance to the 5' flanking gene (start and end position) and to the 3' flanking gene and then used the minimum of these 4 values. If the SNP fell within the transcribed region of a gene, the distance was 0.

Estimating probability of observed and expected overlap between a regulatory feature and GWAS locus

We estimated the probability that a set of GWAS loci overlap with a regulatory feature more often than we expect by chance using the following method. We considered a GWAS locus as the GWAS index SNP or a SNP in LD with the index SNP ($r^2 > 0.7$). For each regulatory feature, we counted the number of GWAS loci in which we observed physical overlap with at least one experimentally defined genomic region of the feature. The number of GWAS index SNPs in the i th matched control set that demonstrates positional overlap with a given epigenomic feature, written as s_i , follows a binomial distribution with parameters n_i and p_i . The parameter n_i is equal to the number of index SNPs present in the i th control set. The second parameter p_i is calculated as the number of variants in the i th control

set or their LD proxies that overlaps with the feature, divided by the total number of variants in the *i*th control set. If we assume there are *r* control sets in total, the number of index SNPs from all control sets that falls in a single feature is the sum of independent non-identical binomial random variables:

$$S = \sum_{i=1}^r s_i$$

In most cases only one index variant is assigned to a matched control set, but there are some exceptions where more than one index SNP could match on the same 3 properties. We estimate an enrichment P-value for any given *s* as $P(S \geq s)$. *P* is the cumulative right tail probability based on the distribution of *S* and is calculated using a saddlepoint approximation method (Te Grotenhuis, et al., 2013).

Permutation testing to evaluate estimated P-values

We performed up to 100,000 permutations to evaluate our enrichment P-value estimation method and found the results to be highly concordant for permutation P-values less than 1×10^{-5} that could be estimated (**Figure S3**). To assess the expected overlap with a regulatory domain, we generated 100,000 random permuted sets of non-associated matched control SNPs based on the criteria described above. We selected a control variant from the control pool for each locus and identified the variants in LD, resulting in 100,000 control sets. We evaluated the random SNP lists for overlap with each functional domain by averaging the number of SNPs that fell within the experimentally annotated regions from each control set that had at least one variant overlapping a regulatory element. This approach assumes that only one variant located in a regulatory region at each locus is responsible for the association signal. We calculated an empirical P-value for each regulatory dataset as the proportion of random sets with an equal or greater number of loci overlapping the regulatory domain than the observed set of trait-associated variants. For small P-values that could not be estimated (e.g. $P < 1 \times 10^{-5}$ for 100,000 permutations), we used a normal approximation of the empirical overlap distribution to estimate P-values.

Luciferase expression constructs

To characterize the intergenic region around the candidate SNPs, 600-800 bp fragments containing the SNPs from human chromosomes were cloned into the pGL4-Promoter vector (Promega), in the 5'-to-3' orientation (toward the GWAS candidate gene), upstream of the firefly luciferase gene (**Table S6**). The QuikChange Site-Directed Mutagenesis Kit (Stratagene) was used to alter single nucleotides at the targeted SNP sites. All constructs were verified by DNA sequencing.

Luciferase expression assays

HepG2 cultured human hepatoma cells were transfected at roughly 50% confluence and maintained in DMEM with 10% FBS. The firefly luciferase constructs were co-transfected with either the C/EBP-β expression plasmid (pcDNA3.1-C/EBP-β) or empty pcDNA3.1 vector, together with the Renilla luciferase pRL-null Vector (Promega) as internal control, using the Lipofectamine 2000 transfection reagent (Invitrogen) in the ratio 0.25 µg:0.25ug:25 ng:2.5 µl mixed with Opti-MEM I Reduced Serum Medium

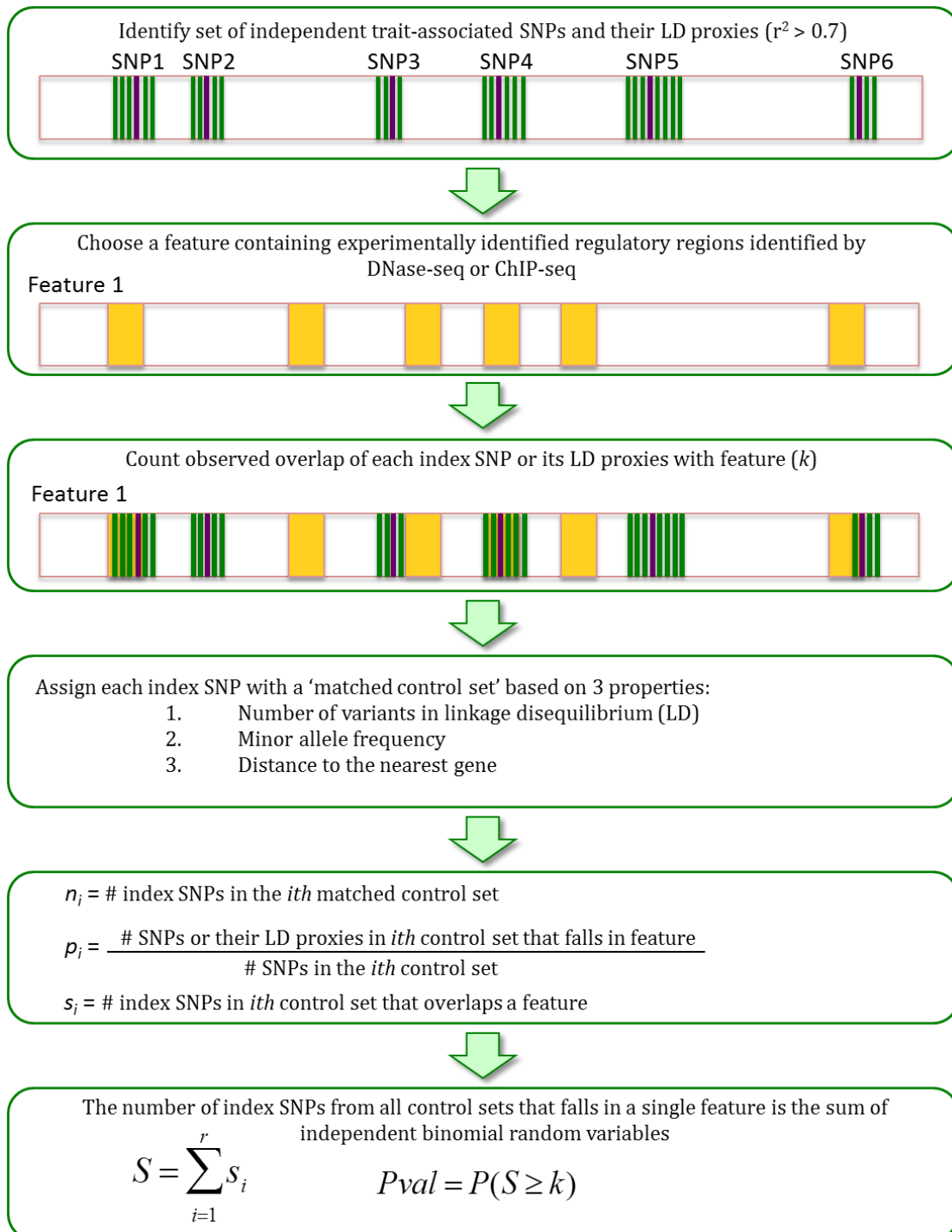
(Invitrogen) for a 50 µl mix used for each well of 24-well plates. Forty-eight hours after transfection, firefly and Renilla luciferase activities were measured using the Dual-Luciferase Reporter Assay System (Promega) according to the manufacturer's protocol, using untransfected cells to adjust for background activity.

Data Access

GREGOR documentation and software download, <http://genome.sph.umich.edu/wiki/GREGOR>; ENCODE Consortium, <http://genome.ucsc.edu/ENCODE/dataMatrix/encodeDataMatrixHuman.html>; Chromatin state segmentation by HMM from ENCODE/Broad in 9 human cell types, <http://genome.ucsc.edu/cgi-bin/hgFileUi?g=wgEncodeBroadHmm&db=hg19>; GWAS results for all traits and diseases including those studied here, <http://www.genome.gov/gwastudies/>. Data from the latest blood pressure study are not yet published; author CJW may be contacted at cristen@umich.edu.

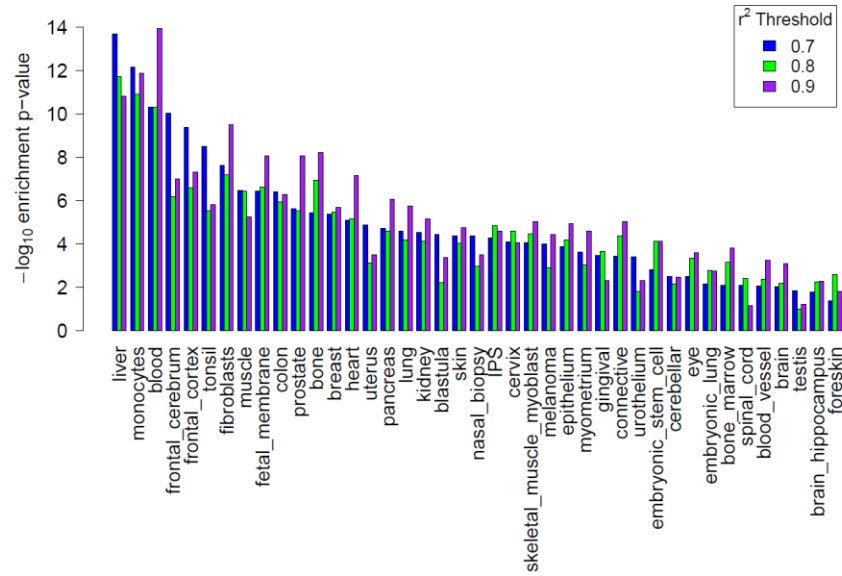
SUPPLEMENTARY FIGURES

Supplementary Figure 1. Summary of GREGOR variant enrichment method.

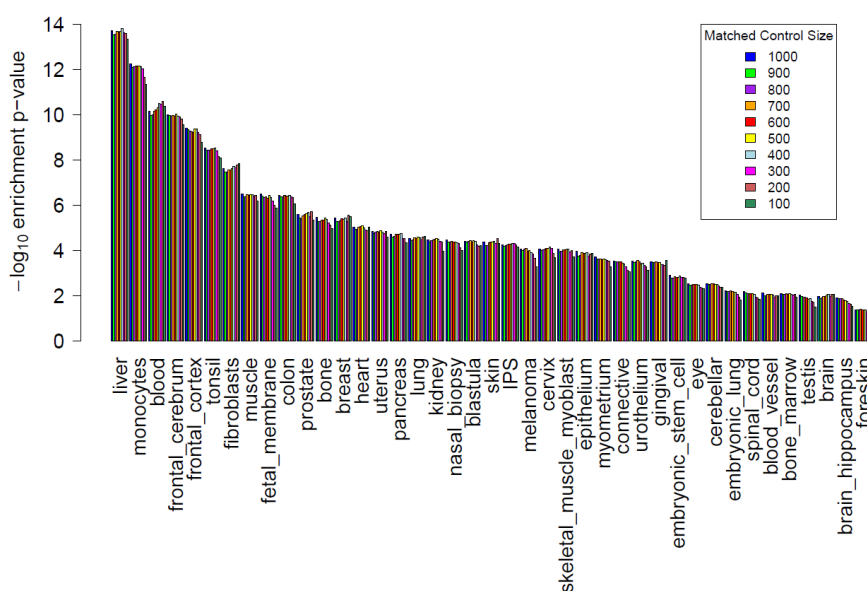


Supplementary Figure 2. Enrichment of lipid-associated variation in DNase hypersensitive sites using different parameter values. Tissues are ordered by decreasing *P*-value significance when using the parameters $r^2 = 0.7$ and matched control set size of 500.

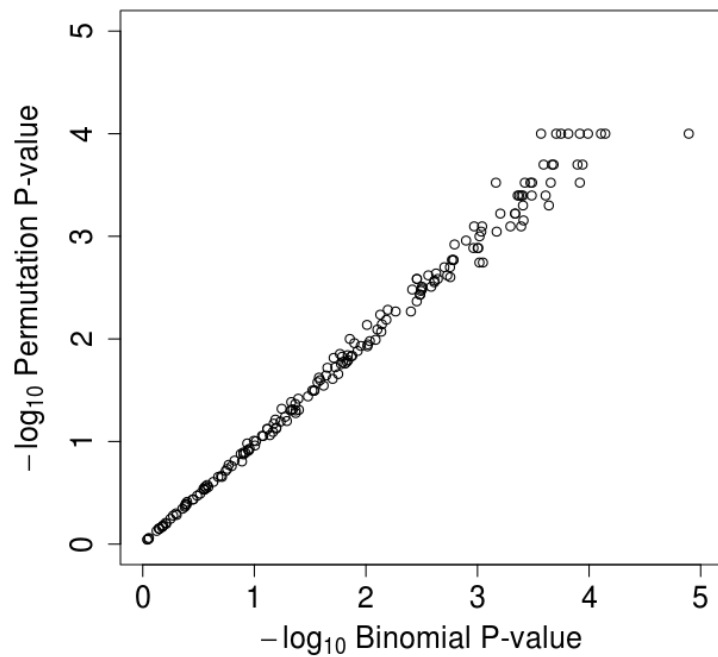
- A. Magnitude of enrichment for a range of r^2 thresholds. The r^2 thresholds were used to select i. the potential functional variants in LD with index variants using 1000 Genomes CEU and ii. The control SNPs with approximately the same number of variants in LD as index variants (using the same threshold as in i). The higher the r^2 value, the fewer variants in LD would be selected.



- B. Magnitude of enrichment for matched control sets of various sizes. Matched control sets contain variants that share the properties of 1) number of LD proxies, 2) minor allele frequency, and 3) gene proximity. The more variants selected as controls, the less close the matching.

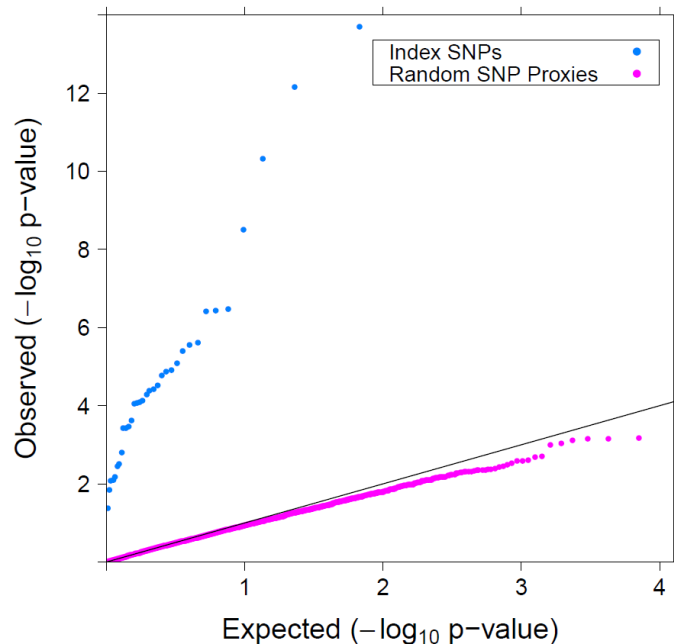


Supplementary Figure 3. Enrichment P -values estimated using 10,000 permutations (y-axis) and the sum of binomial trials as implemented in GREGOR (x-axis) show high concordance. P -values less than 1×10^{-5} cannot be precisely estimated by permutation testing, and so are excluded from the figure.

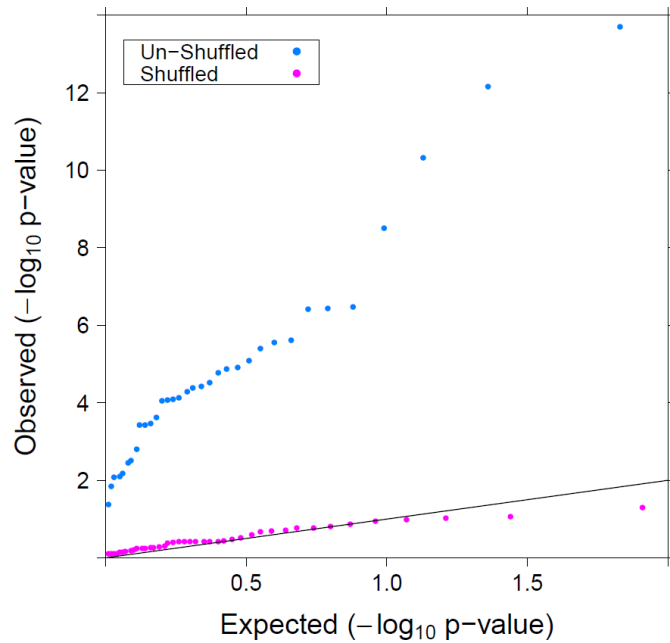


Supplementary Figure 4. QQ plots of enrichment performance for lipid-associated variation in DNase hypersensitive sites and control sets.

- A. Permutation of index variants: A set of 50 lists of ‘SNP proxies’ was generated, where each list contained SNPs that match the lipid-associated SNPs on 3 properties: 1) number of LD proxies, 2) minor allele frequency, and 3) gene proximity but were otherwise randomly selected from across the genome. Enrichment P -values were calculated for each list and are shown in the pink distribution.

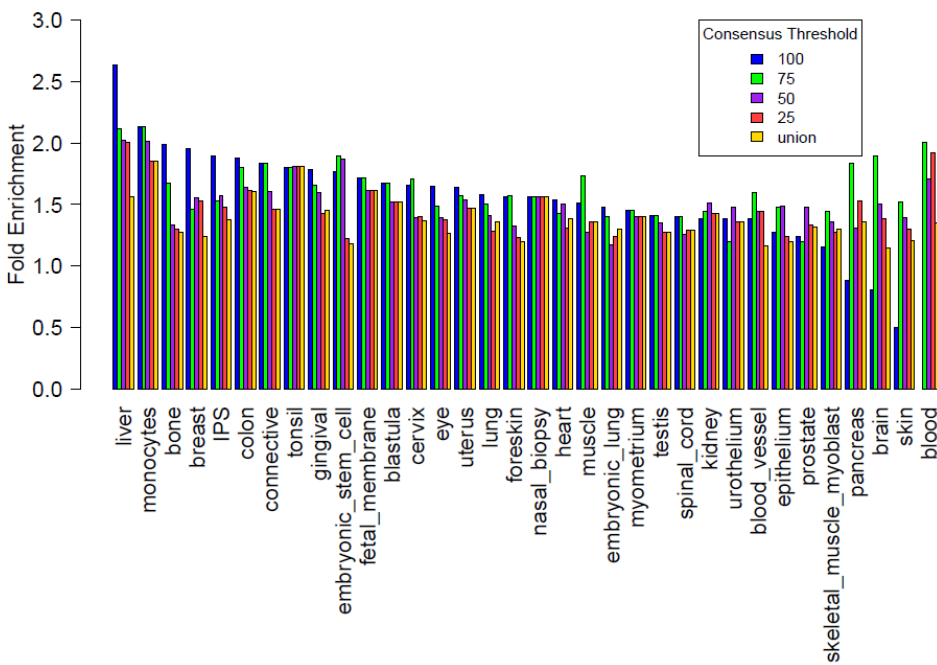


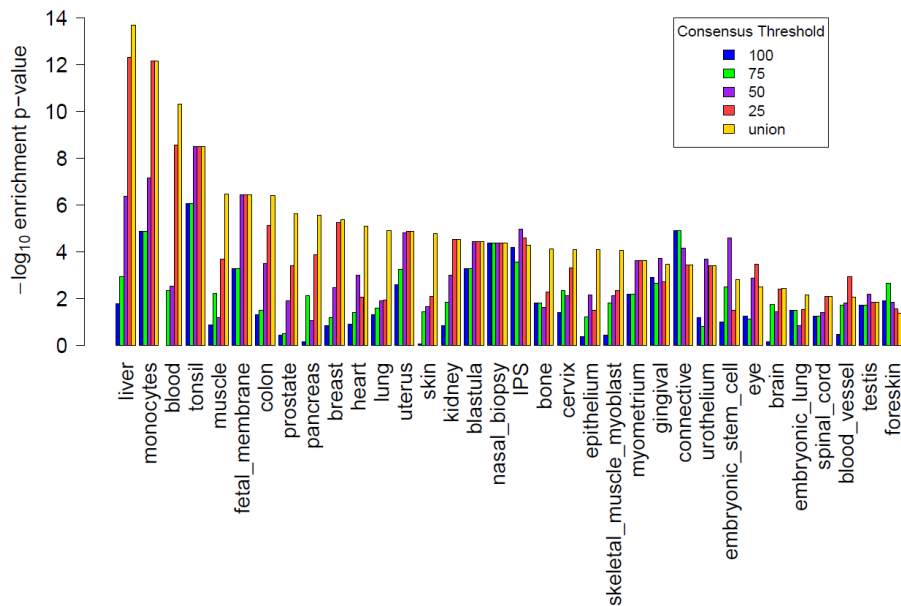
- B. Shuffling of DHSs partitioned by genic landmark categories: We investigated type I error by categorizing DHSs using a hierarchical partitioning approach (Parker, et al., 2013). DHSs were partitioned into mutually exclusive genic landmark categories based on GENCODE annotation (e.g. 3'UTR, 5'UTR, intron, coding exons, intergenic TSS distal and proximal). We randomly shuffled DHSs within each of these categories, and then re-combined them for enrichment analysis. We evaluated the enrichment P -value distribution of lipid-associated variants in DHSs of these partitioned-then-shuffled DHSs (pink) and compared it with the P -value distribution in the original DHSs (blue). By this approach, we still see compelling type I error while maintaining the relationship between gene proximity and DHSs.



Supplementary Figure 5. Fold enrichment (A) and enrichment *P*-values (B) for lipid-associated variation in DNase hypersensitive sites (DHSs) of different tissues and at different ‘consensus thresholds’. A consensus threshold is defined as the percentage of shared DHS regions among cell types derived from a given tissue.

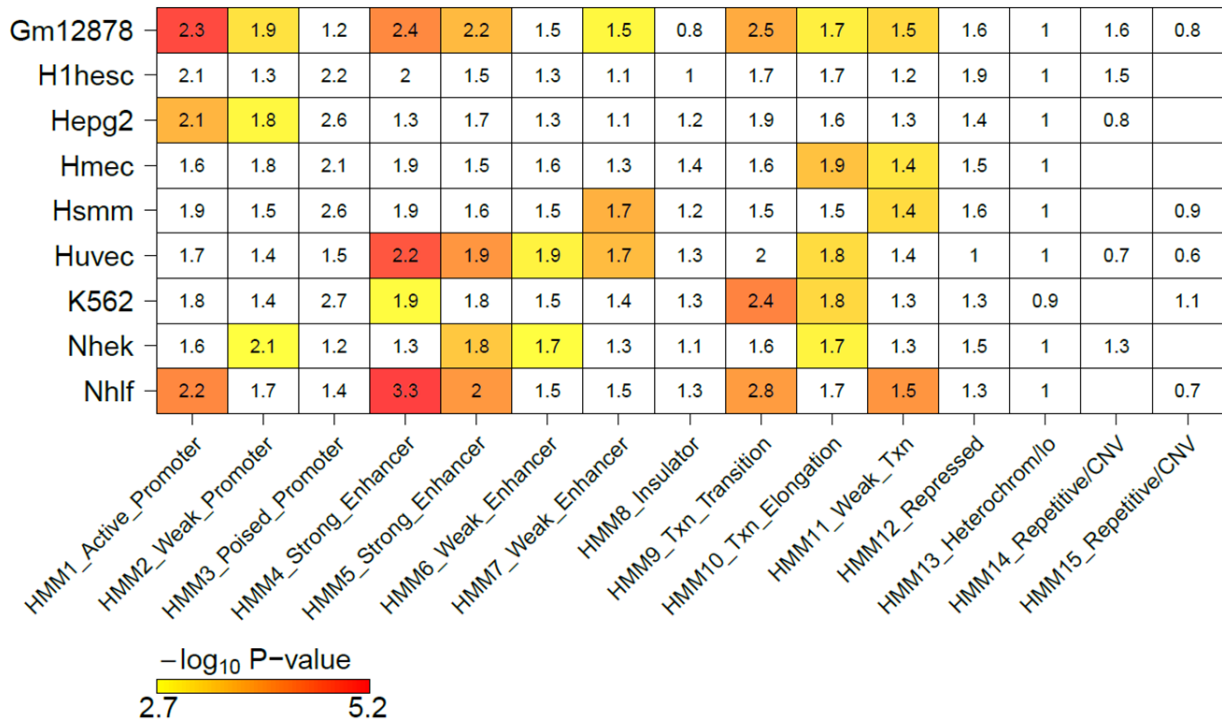
A. Fold Enrichment

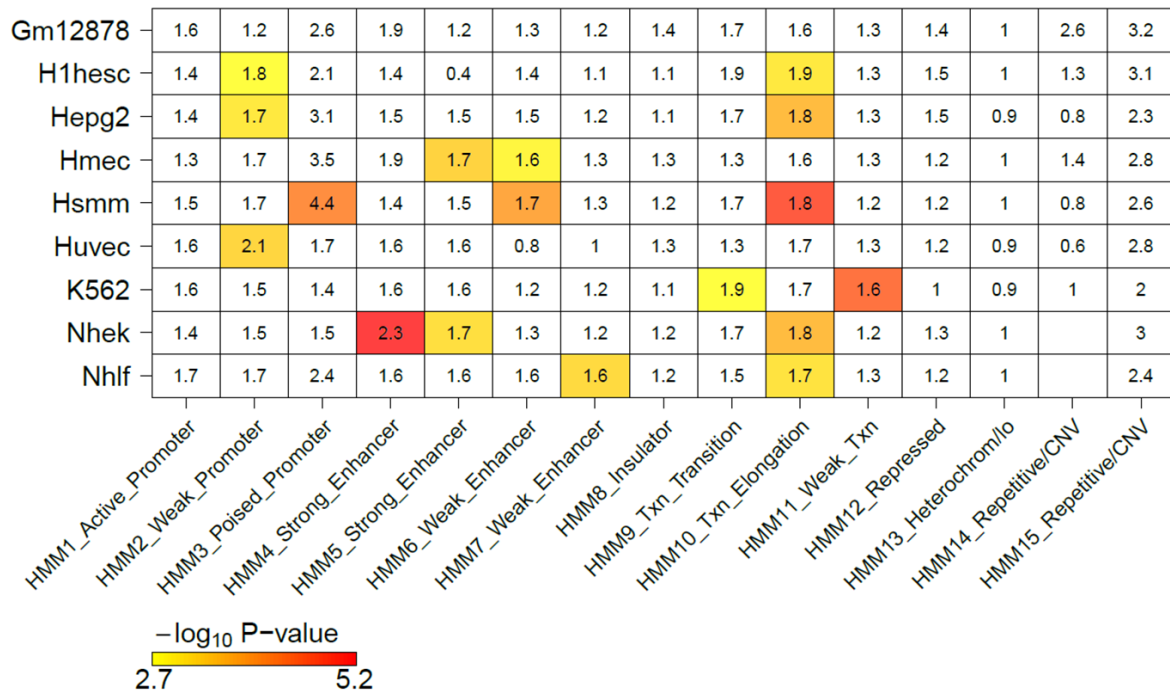
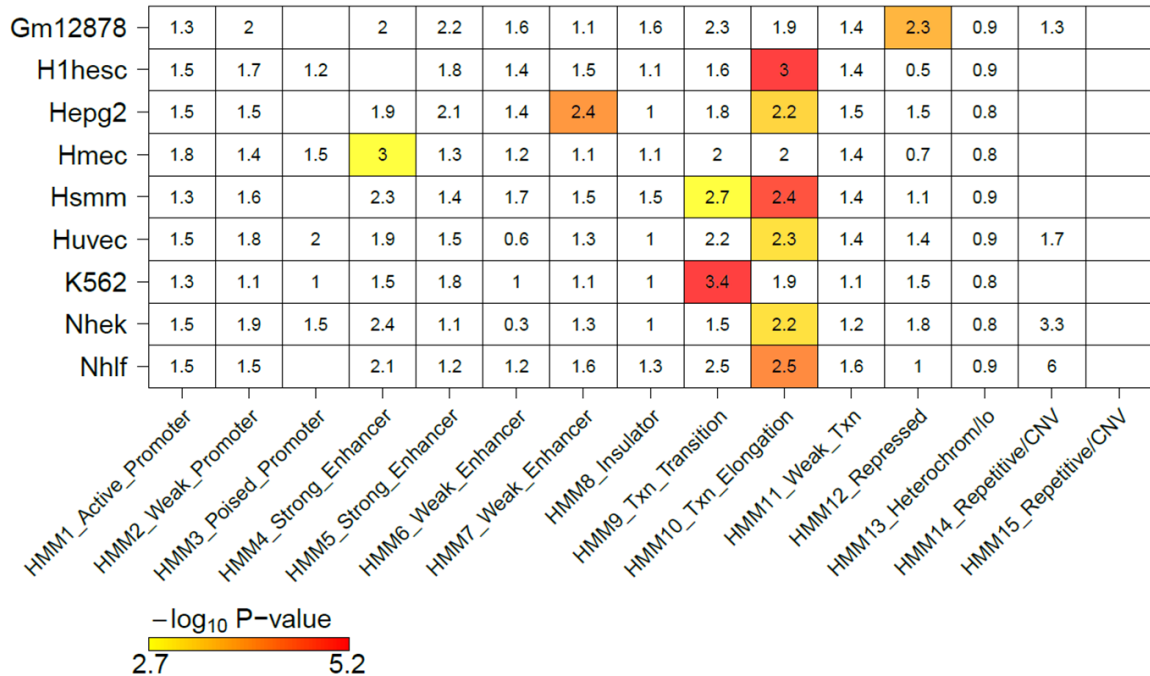


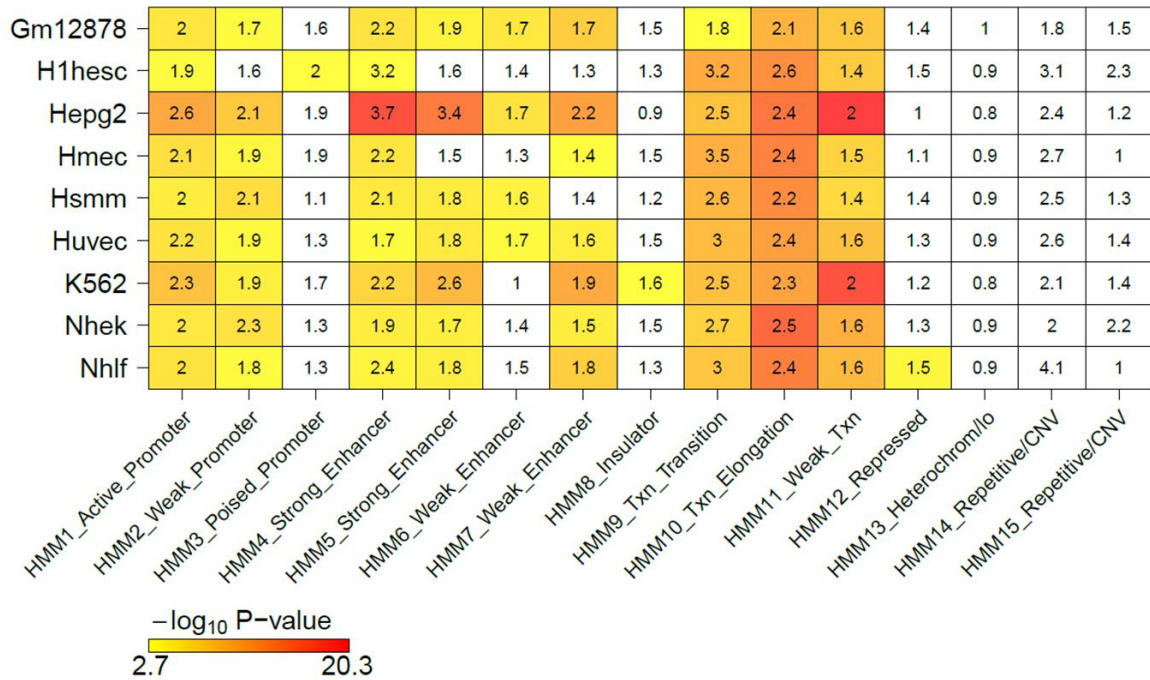
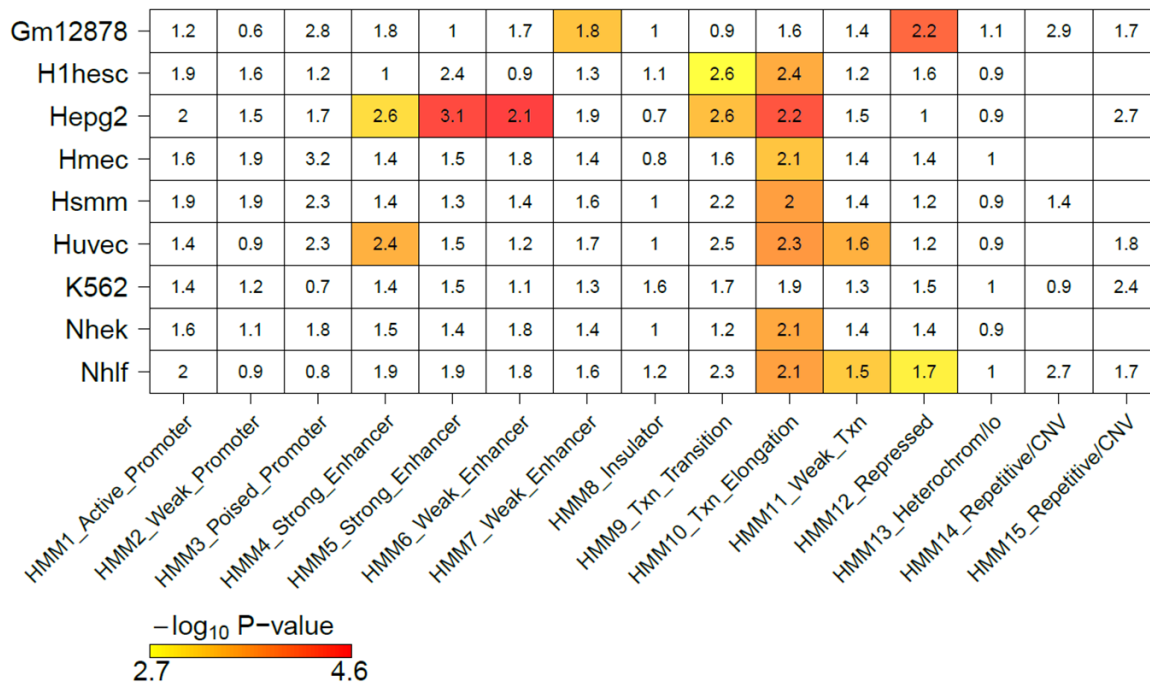
B. Enrichment *P*-values

Supplementary Figure 6. Matrix of fold enrichment for five sets of trait-associated variants in predicted chromatin states in nine human cell types (HMM, hidden Markov model; txn, transcription; lo, low signal; CNV, copy number variation) (Ernst, et al., 2011). Boxes are colored by $-\log_{10}$ enrichment P -value. White color indicates not significant after Bonferroni correction for 15 chromatin states and 9 tissues.

A. Blood Pressure GWAS variants (n=99)



B. Body Mass Index GWAS variants (n=97)**C.** Coronary Artery Disease GWAS variants (n=36)

D. Lipids GWAS variants (n=157)**E. Type 2 Diabetes GWAS variants (n=65)**

Supplementary Figure 7. Prioritization of lipid-associated loci for functional follow-up. Prioritization is based on functional annotation, physical overlap with regulatory domains, and association with transcript levels in relevant tissues. Each expression quantitative trait locus (eQTL) contains at least one variant associated with expression level changes in either liver, omental fat, or subcutaneous fat (eQTL $P < 1 \times 10^{-3}$).

Lipid-associated loci reported from GWAS (Willer et al., 2013) ($n=157$)



Loci without any non-synonymous SNPs in LD ($r^2 > 0.7$) with index SNP ($n=103$)



Loci containing at least one SNP that overlaps with at least 10% of significantly enriched TFBSSs or histone marks ($n=23$)



Loci with less than 32 SNPs ($n=14$)



Loci that contain an eQTL and/or a SNP that overlaps with at least 25% of significantly enriched lipid-related features ($n=11$)

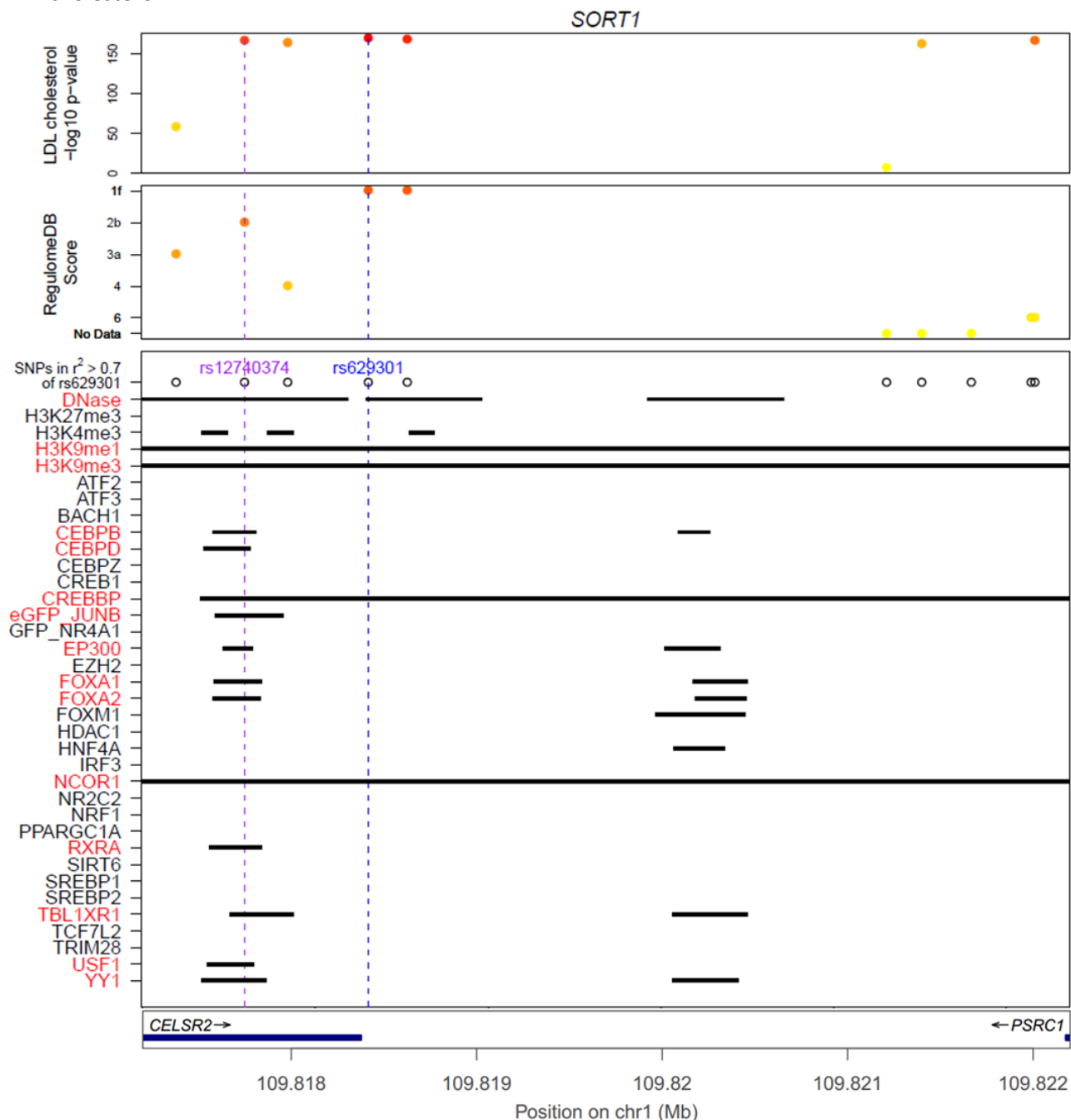


Positive control *SORT1* and randomly selected set of 5 additional loci:

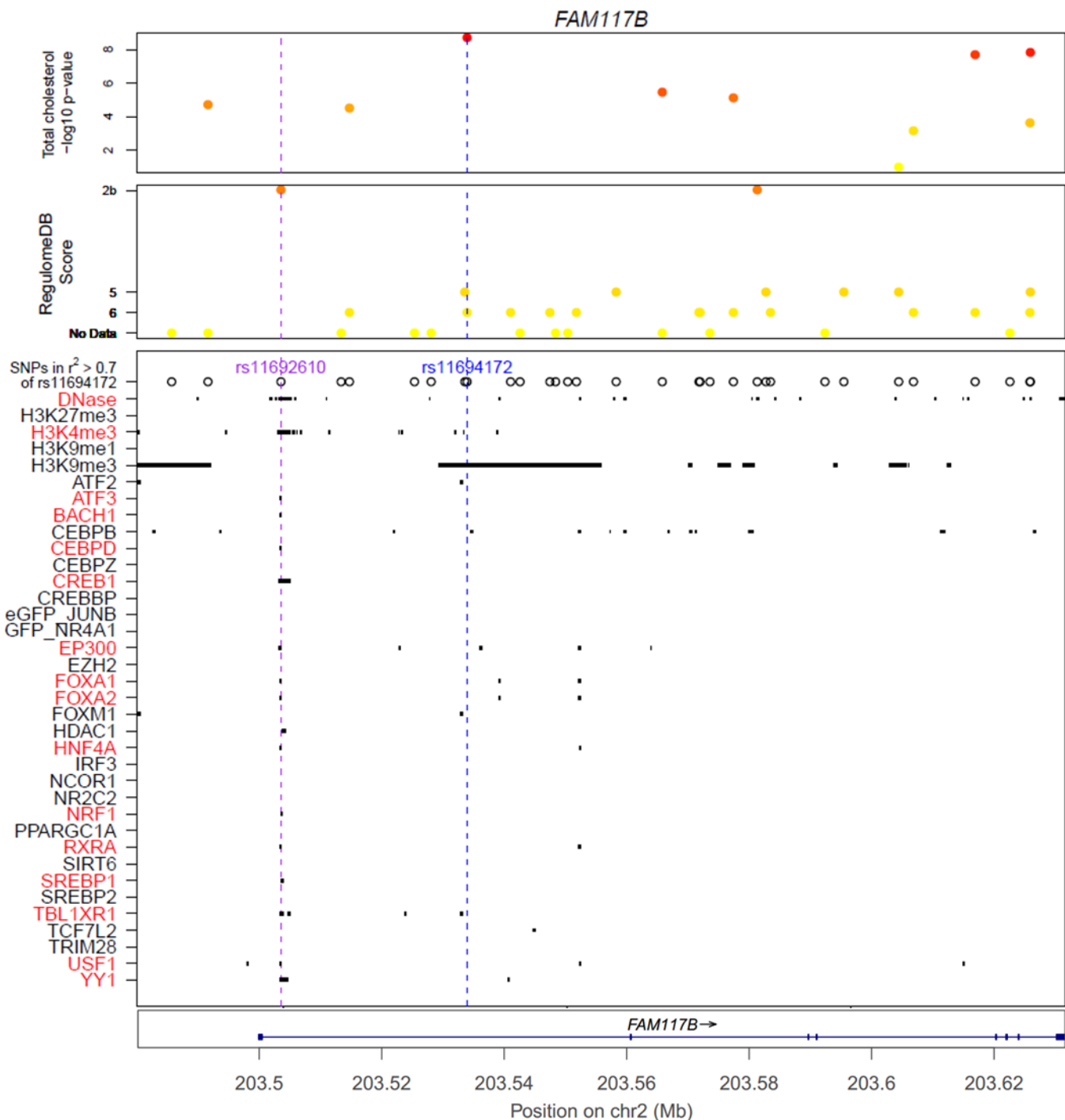
ADH5, SPTLC3, ANGPTL8, FAM117B, IRF2BP2

Supplementary Figure 8. Physical overlap of variants at six lipid loci (SNPs within $r^2 > 0.7$ of the GWAS index SNP) with ChIP-seq or DNase-seq binding sites for lipid-related ENCODE features (The ENCODE Project Consortium, 2012). GWAS $-\log_{10} P$ -values are plotted in the top panel (Teslovich, et al., 2010). RegulomeDB SNP annotation scores of predicted regulatory elements are shown in the second panel (Boyle, et al., 2012). Purple dotted lines annotate the hypothesized functional variant based on physical overlap prediction. Blue dotted lines annotate the control SNP, which is usually the top most significant GWAS SNP. Regulatory elements highlighted in red annotate overlap with the candidate functional variant.

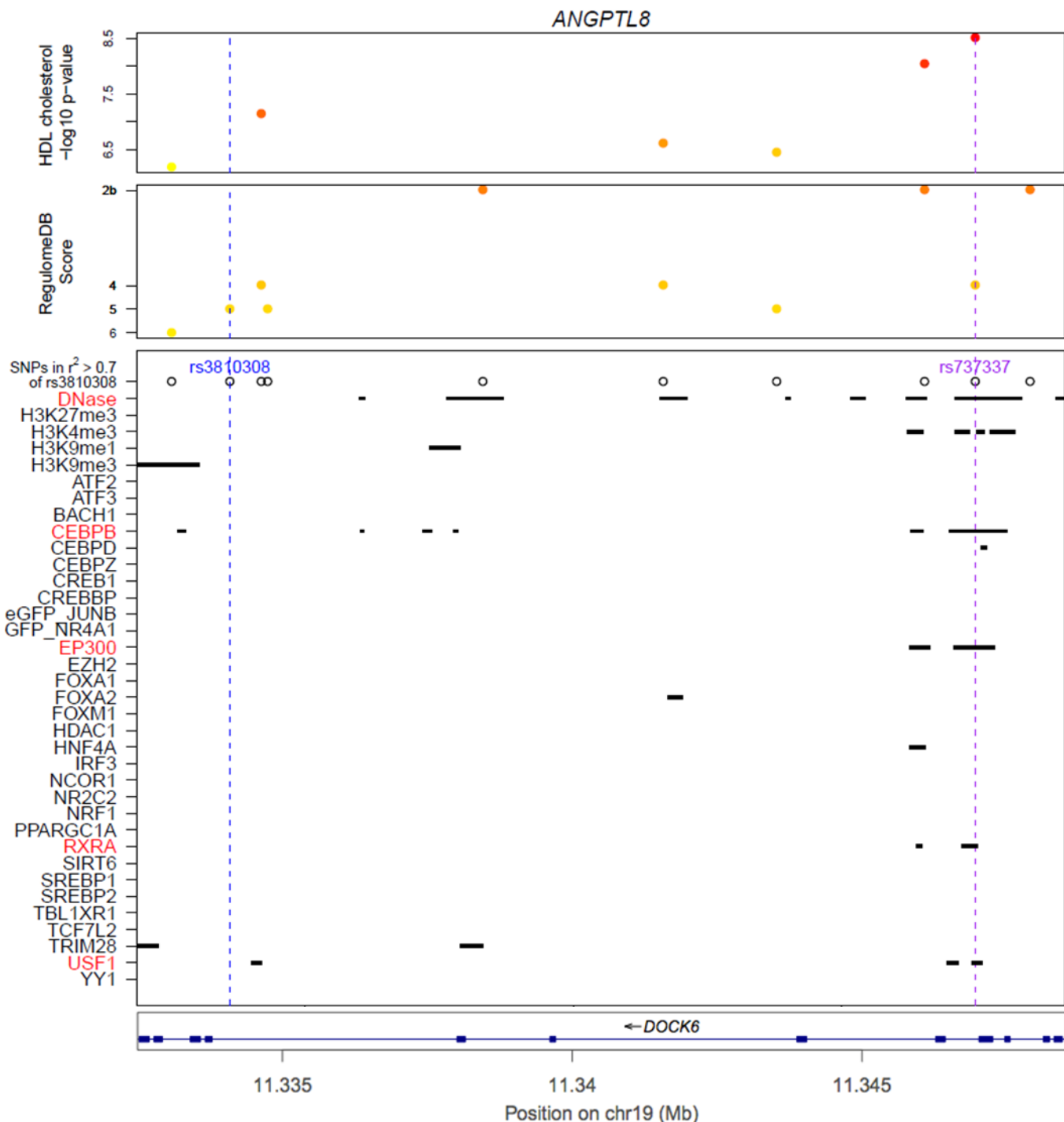
A. ***SORT1* (sortilin 1)**. GWAS index SNP rs629301 is associated with LDL cholesterol and total cholesterol.



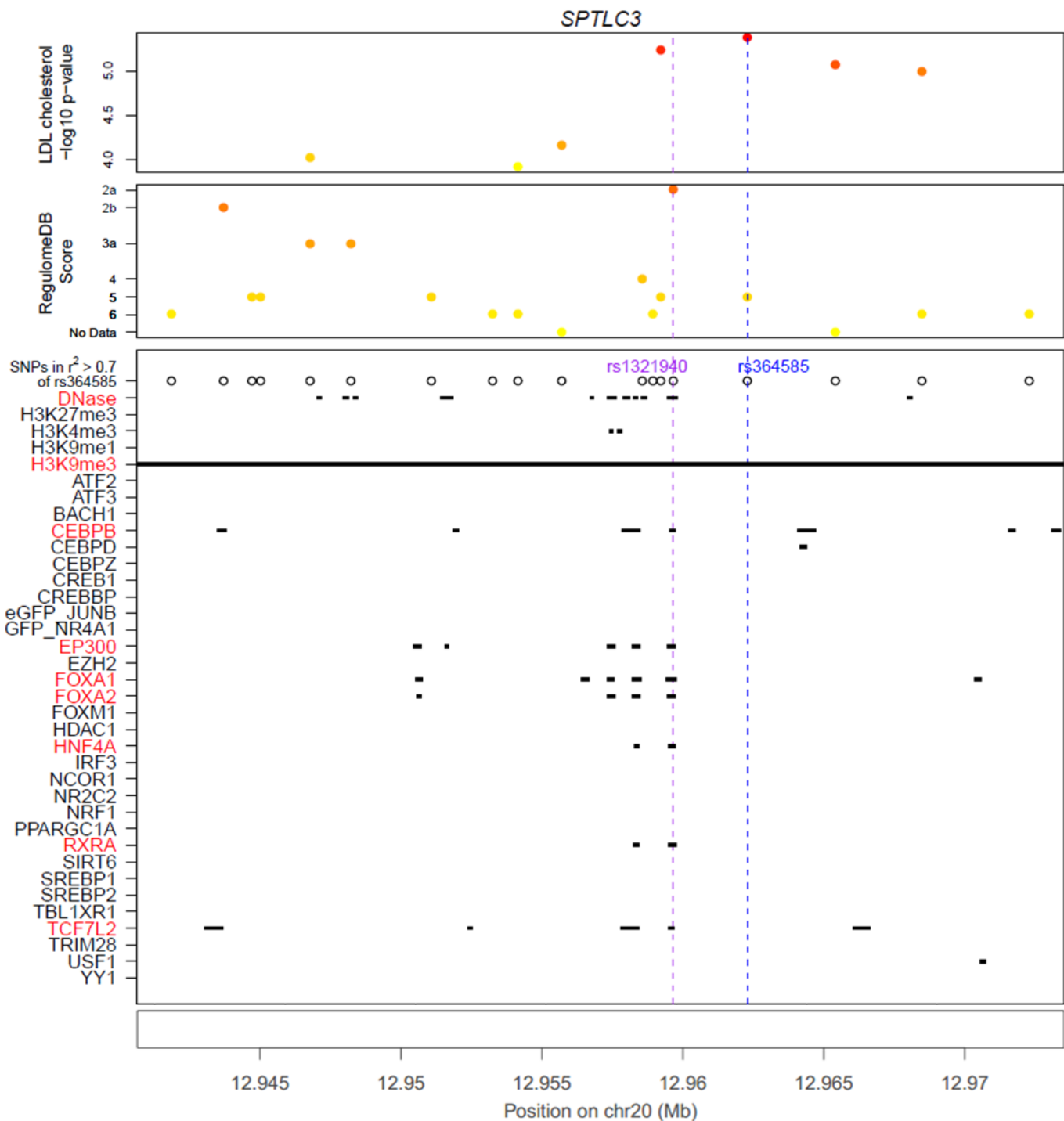
B. ***FAM117B* (family with sequence similarity 117, member B).** GWAS index SNP rs11694172 is associated with total cholesterol.



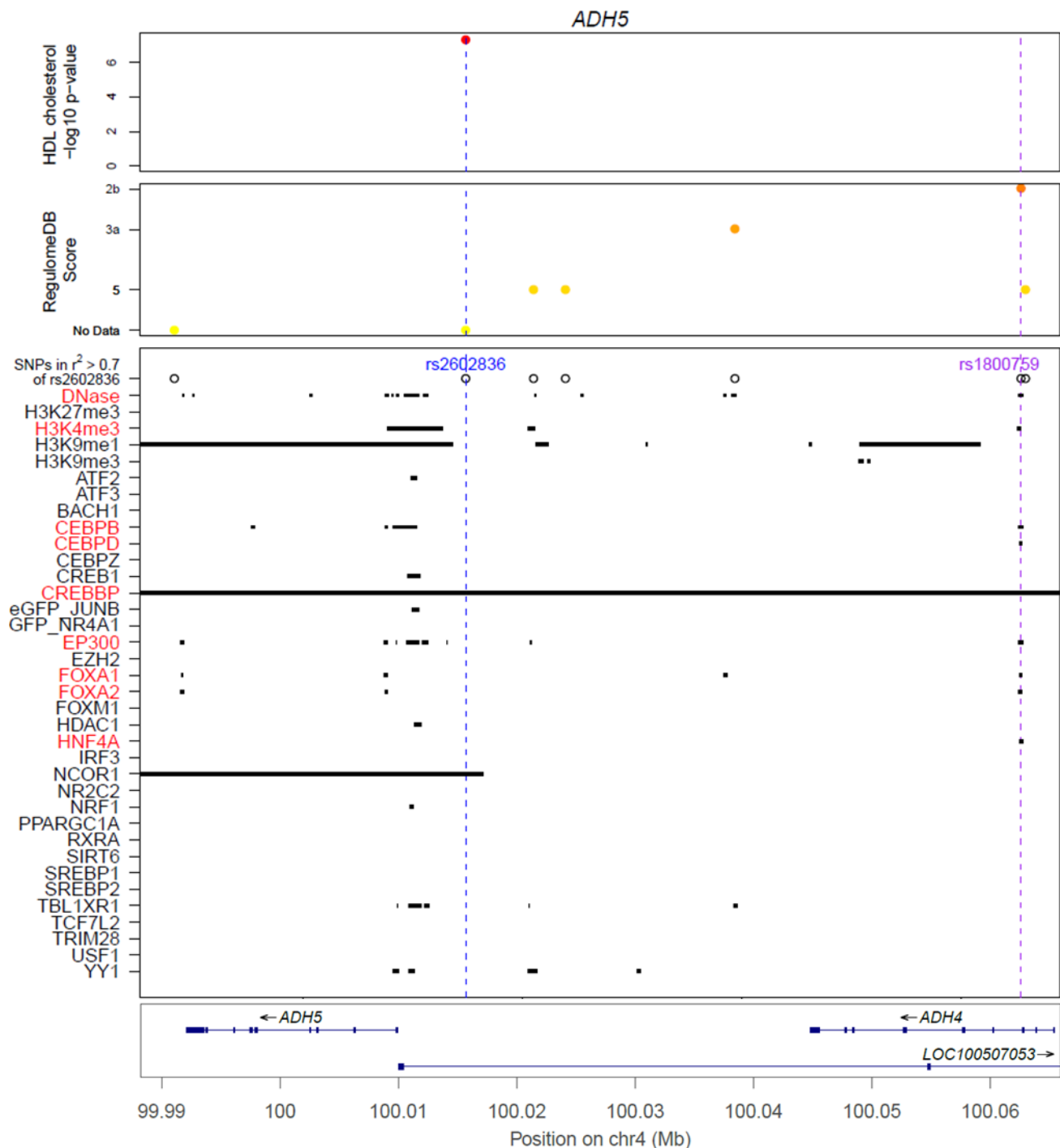
C. ***ANGPTL8* (Angiopoietin-like protein 8; C19orf80: chromosome 19 open reading frame 80).** GWAS index SNP rs737337 is associated with HDL cholesterol, and the candidate functional SNP.



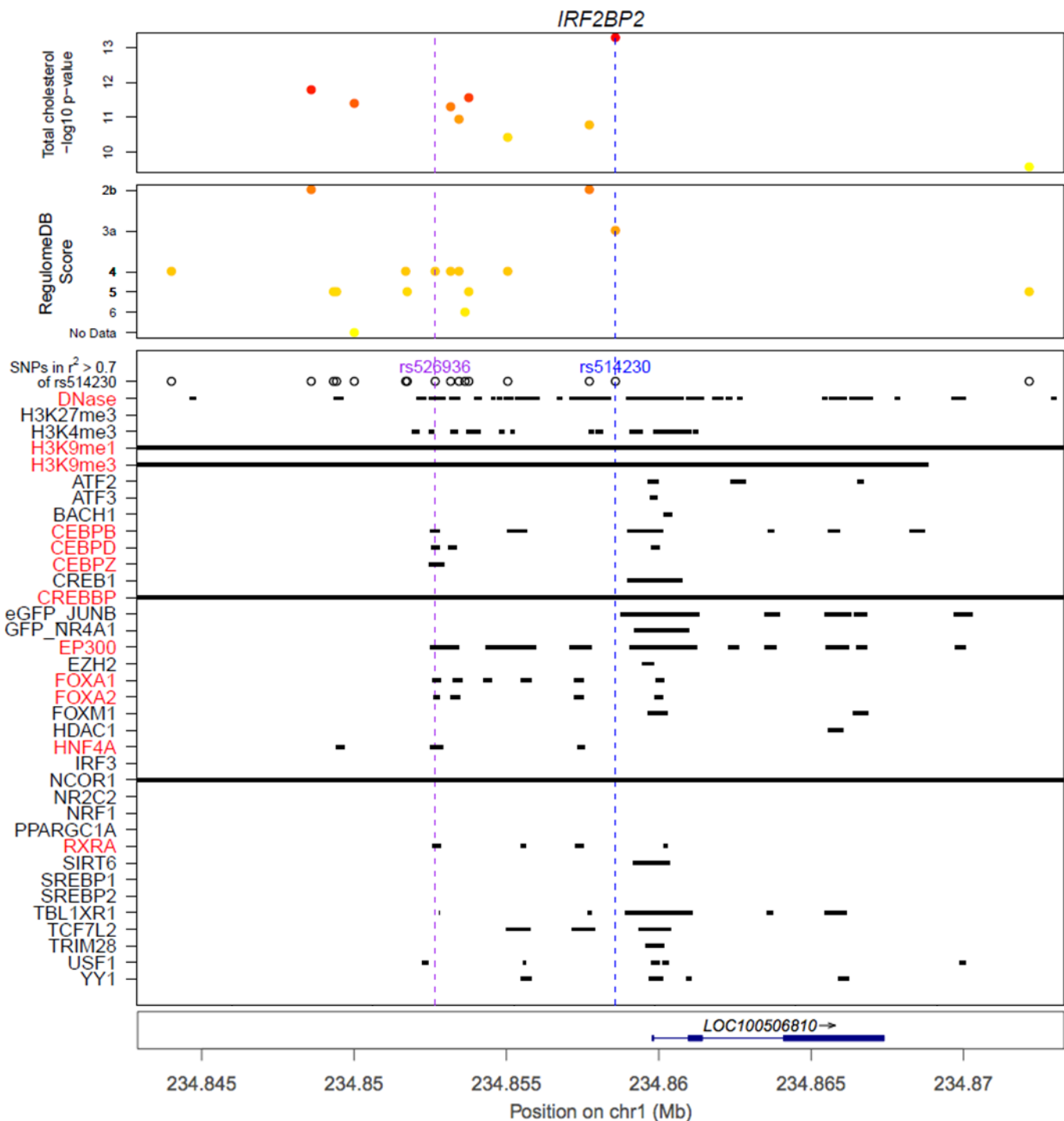
D. ***SPTLC3* (serine palmitoyltransferase, long chain base subunit 3)**. GWAS index SNP rs364585 is associated with LDL cholesterol.



E. ***ADH5* (alcohol dehydrogenase 5 (class III), chi polypeptide).** GWAS index SNP rs2602836 is associated with HDL cholesterol. GWAS *P*-values here are reported from (Willer, et al., 2013).



F. ***IRF2BP2* (interferon regulatory factor 2 binding protein 2)**. GWAS index SNP rs514230 is associated with total cholesterol and LDL cholesterol.



SUPPLEMENTARY TABLES

Supplementary Table 1. ENCODE DNase hypersensitivity sites from various tissues are categorized into broader tissue groups for enrichment analysis.

| broad_tissue_category | ENCODE_tissue_category | BED_File |
|-----------------------|------------------------|---|
| blastula | blastula | wgEncodeAwgDnaseDukeHtr8svnUniPk.narrowPeak |
| blastula | blastula | wgEncodeOpenChromDnaseHtr8Pk.narrowPeak |
| blood | blood | wgEncodeAwgDnaseDukeCllUniPk.narrowPeak |
| blood | blood | wgEncodeAwgDnaseDukeGm12891UniPk.narrowPeak |
| blood | blood | wgEncodeAwgDnaseDukeGm12892UniPk.narrowPeak |
| blood | blood | wgEncodeAwgDnaseDukeGm18507UniPk.narrowPeak |
| blood | blood | wgEncodeAwgDnaseDukeGm19238UniPk.narrowPeak |
| blood | blood | wgEncodeAwgDnaseDukeGm19239UniPk.narrowPeak |
| blood | blood | wgEncodeAwgDnaseDukeGm19240UniPk.narrowPeak |
| blood | blood | wgEncodeAwgDnaseDukeTh0UniPk.narrowPeak |
| blood | blood | wgEncodeAwgDnaseUwCd20UniPk.narrowPeak |
| blood | blood | wgEncodeAwgDnaseUwCd34mobilizedUniPk.narrowPeak |
| blood | blood | wgEncodeAwgDnaseUwCmkUniPk.narrowPeak |
| blood | blood | wgEncodeAwgDnaseUwdukeGm12878UniPk.narrowPeak |
| blood | blood | wgEncodeAwgDnaseUwdukeK562UniPk.narrowPeak |
| blood | blood | wgEncodeAwgDnaseUwdukeTh1UniPk.narrowPeak |
| blood | blood | wgEncodeAwgDnaseUwGm06990UniPk.narrowPeak |
| blood | blood | wgEncodeAwgDnaseUwGm12864UniPk.narrowPeak |
| blood | blood | wgEncodeAwgDnaseUwGm12865UniPk.narrowPeak |
| blood | blood | wgEncodeAwgDnaseUwHl60UniPk.narrowPeak |
| blood | blood | wgEncodeAwgDnaseUwJurkatUniPk.narrowPeak |
| blood | blood | wgEncodeAwgDnaseUwNb4UniPk.narrowPeak |
| blood | blood | wgEncodeAwgDnaseUwTh2UniPk.narrowPeak |
| blood | blood | wgEncodeOpenChromDnaseAdultcd4th0Pk.narrowPeak |
| blood | blood | wgEncodeOpenChromDnaseAdultcd4th1Pk.narrowPeak |
| blood | blood | wgEncodeOpenChromDnaseCd20ro01794Pk.narrowPeak |

Enrichment of GWAS variants in epigenomic features

| | | |
|-------|-------|--|
| blood | blood | wgEncodeOpenChromDnaseClIPk.narrowPeak |
| blood | blood | wgEncodeOpenChromDnaseGm10248Pk.narrowPeak |
| blood | blood | wgEncodeOpenChromDnaseGm10266Pk.narrowPeak |
| blood | blood | wgEncodeOpenChromDnaseGm12878Pk.narrowPeak |
| blood | blood | wgEncodeOpenChromDnaseGm12891Pk.narrowPeak |
| blood | blood | wgEncodeOpenChromDnaseGm12892Pk.narrowPeak |
| blood | blood | wgEncodeOpenChromDnaseGm13976Pk.narrowPeak |
| blood | blood | wgEncodeOpenChromDnaseGm13977Pk.narrowPeak |
| blood | blood | wgEncodeOpenChromDnaseGm18507Pk.narrowPeak |
| blood | blood | wgEncodeOpenChromDnaseGm19238Pk.narrowPeak |
| blood | blood | wgEncodeOpenChromDnaseGm19239Pk.narrowPeak |
| blood | blood | wgEncodeOpenChromDnaseGm19240Pk.narrowPeak |
| blood | blood | wgEncodeOpenChromDnaseGm20000Pk.narrowPeak |
| blood | blood | wgEncodeOpenChromDnaseK562G1phasePk.narrowPeak |
| blood | blood | wgEncodeOpenChromDnaseK562G2mphasePk.narrowPeak |
| blood | blood | wgEncodeOpenChromDnaseK562NabutPk.narrowPeak |
| blood | blood | wgEncodeOpenChromDnaseK562PkV2.narrowPeak |
| blood | blood | wgEncodeOpenChromDnaseK562Saha1u72hrPk.narrowPeak |
| blood | blood | wgEncodeOpenChromDnaseK562SahactrlPk.narrowPeak |
| blood | blood | wgEncodeUwDnaseCd20ro01778PkRep1.narrowPeak |
| blood | blood | wgEncodeUwDnaseCd20ro01778PkRep2.narrowPeak |
| blood | blood | wgEncodeUwDnaseCd34mobilizedPkRep1.narrowPeak |
| blood | blood | wgEncodeUwDnaseCd4naivewb11970640PkRep1.narrowPeak |
| blood | blood | wgEncodeUwDnaseCd4naivewb78495824PkRep1.narrowPeak |
| blood | blood | wgEncodeUwDnaseCmkPkRep1.narrowPeak |
| blood | blood | wgEncodeUwDnaseGm06990PkRep1.narrowPeak |
| blood | blood | wgEncodeUwDnaseGm06990PkRep2.narrowPeak |
| blood | blood | wgEncodeUwDnaseGm12864PkRep1.narrowPeak |
| blood | blood | wgEncodeUwDnaseGm12865PkRep1.narrowPeak |
| blood | blood | wgEncodeUwDnaseGm12865PkRep2.narrowPeak |
| blood | blood | wgEncodeUwDnaseGm12878PkRep1.narrowPeak |
| blood | blood | wgEncodeUwDnaseGm12878PkRep2.narrowPeak |
| blood | blood | wgEncodeUwDnaseHl60PkRep1.narrowPeak |

Enrichment of GWAS variants in epigenomic features

| | | |
|--------------|--------------|--|
| blood | blood | wgEncodeUwDnaseH160PkRep2.narrowPeak |
| blood | blood | wgEncodeUwDnaseJurkatPkRep1.narrowPeak |
| blood | blood | wgEncodeUwDnaseJurkatPkRep2.narrowPeak |
| blood | blood | wgEncodeUwDnaseK562PkRep1.narrowPeak |
| blood | blood | wgEncodeUwDnaseK562PkRep2.narrowPeak |
| blood | blood | wgEncodeUwDnaseNb4PkRep1.narrowPeak |
| blood | blood | wgEncodeUwDnaseNb4PkRep2.narrowPeak |
| blood | blood | wgEncodeUwDnaseTh17PkRep1.narrowPeak |
| blood | blood | wgEncodeUwDnaseTh1PkRep1.narrowPeak |
| blood | blood | wgEncodeUwDnaseTh1PkRep2.narrowPeak |
| blood | blood | wgEncodeUwDnaseTh1wb33676984PkRep1.narrowPeak |
| blood | blood | wgEncodeUwDnaseTh1wb54553204PkRep1.narrowPeak |
| blood | blood | wgEncodeUwDnaseTh1wb54553204PkRep2.narrowPeak |
| blood | blood | wgEncodeUwDnaseTh2PkRep1.narrowPeak |
| blood | blood | wgEncodeUwDnaseTh2PkRep2.narrowPeak |
| blood | blood | wgEncodeUwDnaseTh2wb33676984PkRep1.narrowPeak |
| blood | blood | wgEncodeUwDnaseTh2wb54553204PkRep1.narrowPeak |
| blood | blood | wgEncodeUwDnaseTregwb78495824PkRep1.narrowPeak |
| blood | blood | wgEncodeUwDnaseTregwb83319432PkRep1.narrowPeak |
| blood_vessel | blood_vessel | wgEncodeAwgDnaseDukeAosmcUniPk.narrowPeak |
| blood_vessel | blood_vessel | wgEncodeAwgDnaseUwAoafUniPk.narrowPeak |
| blood_vessel | blood_vessel | wgEncodeAwgDnaseUwdukeHuvecUniPk.narrowPeak |
| blood_vessel | blood_vessel | wgEncodeAwgDnaseUwHbmecUniPk.narrowPeak |
| blood_vessel | blood_vessel | wgEncodeAwgDnaseUwHmvecdadUniPk.narrowPeak |
| blood_vessel | blood_vessel | wgEncodeAwgDnaseUwHmvecdbladUniPk.narrowPeak |
| blood_vessel | blood_vessel | wgEncodeAwgDnaseUwHmvecdblneoUniPk.narrowPeak |
| blood_vessel | blood_vessel | wgEncodeAwgDnaseUwHmvecdlyadUniPk.narrowPeak |
| blood_vessel | blood_vessel | wgEncodeAwgDnaseUwHmvecdlyneoUniPk.narrowPeak |
| blood_vessel | blood_vessel | wgEncodeAwgDnaseUwHmvecdneoUniPk.narrowPeak |
| blood_vessel | blood_vessel | wgEncodeAwgDnaseUwHmveclblUniPk.narrowPeak |
| blood_vessel | blood_vessel | wgEncodeAwgDnaseUwHmvecllyUniPk.narrowPeak |
| blood_vessel | blood_vessel | wgEncodeAwgDnaseUwHpaecUniPk.narrowPeak |
| blood_vessel | blood_vessel | wgEncodeAwgDnaseUwHpafUniPk.narrowPeak |

Enrichment of GWAS variants in epigenomic features

| | | |
|--------------|--------------|---|
| blood_vessel | blood_vessel | wgEncodeOpenChromDnaseAosmcSerumfreePk.narrowPeak |
| blood_vessel | blood_vessel | wgEncodeOpenChromDnaseHuvecPk.narrowPeak |
| blood_vessel | blood_vessel | wgEncodeUwDnaseAoafPkRep1.narrowPeak |
| blood_vessel | blood_vessel | wgEncodeUwDnaseAoafPkRep2.narrowPeak |
| blood_vessel | blood_vessel | wgEncodeUwDnaseHbmecPkRep1.narrowPeak |
| blood_vessel | blood_vessel | wgEncodeUwDnaseHbmecPkRep2.narrowPeak |
| blood_vessel | blood_vessel | wgEncodeUwDnaseHbvpPkRep1.narrowPeak |
| blood_vessel | blood_vessel | wgEncodeUwDnaseHbvsmpkRep1.narrowPeak |
| blood_vessel | blood_vessel | wgEncodeUwDnaseHbvsmpkRep2.narrowPeak |
| blood_vessel | blood_vessel | wgEncodeUwDnaseHmvecadPkRep1.narrowPeak |
| blood_vessel | blood_vessel | wgEncodeUwDnaseHmvecadPkRep2.narrowPeak |
| blood_vessel | blood_vessel | wgEncodeUwDnaseHmvecdbladPkRep1.narrowPeak |
| blood_vessel | blood_vessel | wgEncodeUwDnaseHmvecdbladPkRep2.narrowPeak |
| blood_vessel | blood_vessel | wgEncodeUwDnaseHmvecdblneoPkRep1.narrowPeak |
| blood_vessel | blood_vessel | wgEncodeUwDnaseHmvecdblneoPkRep2.narrowPeak |
| blood_vessel | blood_vessel | wgEncodeUwDnaseHmvecdlyadPkRep1.narrowPeak |
| blood_vessel | blood_vessel | wgEncodeUwDnaseHmvecdlyadPkRep2.narrowPeak |
| blood_vessel | blood_vessel | wgEncodeUwDnaseHmvecdlyneoPkRep1.narrowPeak |
| blood_vessel | blood_vessel | wgEncodeUwDnaseHmvecdlyneoPkRep2.narrowPeak |
| blood_vessel | blood_vessel | wgEncodeUwDnaseHmvecdneopkRep1.narrowPeak |
| blood_vessel | blood_vessel | wgEncodeUwDnaseHmvecdneopkRep2.narrowPeak |
| blood_vessel | blood_vessel | wgEncodeUwDnaseHmveclblPkRep1.narrowPeak |
| blood_vessel | blood_vessel | wgEncodeUwDnaseHmveclblPkRep2.narrowPeak |
| blood_vessel | blood_vessel | wgEncodeUwDnaseHmvecllyPkRep1.narrowPeak |
| blood_vessel | blood_vessel | wgEncodeUwDnaseHmvecllyPkRep2.narrowPeak |
| blood_vessel | blood_vessel | wgEncodeUwDnaseHpaecPkRep1.narrowPeak |
| blood_vessel | blood_vessel | wgEncodeUwDnaseHpafPkRep1.narrowPeak |
| blood_vessel | blood_vessel | wgEncodeUwDnaseHpafPkRep2.narrowPeak |
| blood_vessel | blood_vessel | wgEncodeUwDnaseHuvecPkRep1V2.narrowPeak |
| blood_vessel | blood_vessel | wgEncodeUwDnaseHuvecPkRep2.narrowPeak |
| bone | bone | wgEncodeAwgDnaseDukeOsteoblUniPk.narrowPeak |
| bone | bone | wgEncodeOpenChromDnaseOsteoblPk.narrowPeak |
| bone_marrow | bone_marrow | wgEncodeUwDnaseHs27aPkRep1.narrowPeak |

Enrichment of GWAS variants in epigenomic features

| | | |
|-------------------|-------------------|--|
| bone_marrow | bone_marrow | wgEncodeUwDnaseHs5PkRep1.narrowPeak |
| bone_marrow | bone_marrow | wgEncodeUwDnaseMscPkRep1.narrowPeak |
| bone_marrow | bone_marrow | wgEncodeUwDnaseMscPkRep2.narrowPeak |
| brain | brain | wgEncodeAwgDnaseDukeGlioblaUniPk.narrowPeak |
| brain | brain | wgEncodeAwgDnaseDukeMedulloUniPk.narrowPeak |
| brain | brain | wgEncodeAwgDnaseUwBe2cUniPk.narrowPeak |
| brain | brain | wgEncodeAwgDnaseUwNhaUniPk.narrowPeak |
| brain | brain | wgEncodeAwgDnaseUwSknmcUniPk.narrowPeak |
| brain | brain | wgEncodeAwgDnaseUwSknshraUniPk.narrowPeak |
| brain | brain | wgEncodeOpenChromDnaseGlioblaPk.narrowPeak |
| brain | brain | wgEncodeOpenChromDnaseMedullo341Pk.narrowPeak |
| brain | brain | wgEncodeOpenChromDnaseMedulloPk.narrowPeak |
| brain | brain | wgEncodeOpenChromDnaseSknshPk.narrowPeak |
| brain | brain | wgEncodeUwDnaseBe2cPkRep1.narrowPeak |
| brain | brain | wgEncodeUwDnaseBe2cPkRep2.narrowPeak |
| brain | brain | wgEncodeUwDnaseM059jPkRep1.narrowPeak |
| brain | brain | wgEncodeUwDnaseM059jPkRep2.narrowPeak |
| brain | brain | wgEncodeUwDnaseNhaPkRep1.narrowPeak |
| brain | brain | wgEncodeUwDnaseNhaPkRep2.narrowPeak |
| brain | brain | wgEncodeUwDnaseSknmcPkRep1.narrowPeak |
| brain | brain | wgEncodeUwDnaseSknmcPkRep2.narrowPeak |
| brain | brain | wgEncodeUwDnaseSknshraPkRep1.narrowPeak |
| brain | brain | wgEncodeUwDnaseSknshraPkRep2.narrowPeak |
| brain_hippocampus | brain_hippocampus | wgEncodeAwgDnaseUwHahUniPk.narrowPeak |
| brain_hippocampus | brain_hippocampus | wgEncodeUwDnaseHahPkRep1.narrowPeak |
| brain_hippocampus | brain_hippocampus | wgEncodeUwDnaseHahPkRep2.narrowPeak |
| breast | breast | wgEncodeAwgDnaseDukeMcf7hypoxiaUniPk.narrowPeak |
| breast | breast | wgEncodeAwgDnaseDukeT47dUniPk.narrowPeak |
| breast | breast | wgEncodeAwgDnaseUwdukeHmecUniPk.narrowPeak |
| breast | breast | wgEncodeAwgDnaseUwdukeMcf7UniPk.narrowPeak |
| breast | breast | wgEncodeOpenChromDnaseHmecPk.narrowPeak |
| breast | breast | wgEncodeOpenChromDnaseMcf7CtcfshrnaPk.narrowPeak |
| breast | breast | wgEncodeOpenChromDnaseMcf7HypoxlacconPk.narrowPeak |

Enrichment of GWAS variants in epigenomic features

| | | |
|------------|------------|---|
| breast | breast | wgEncodeOpenChromDnaseMcf7HypoxlacPk.narrowPeak |
| breast | breast | wgEncodeOpenChromDnaseMcf7Pk.narrowPeak |
| breast | breast | wgEncodeOpenChromDnaseMcf7RandshrnaPk.narrowPeak |
| breast | breast | wgEncodeOpenChromDnaseT47dEst10nm30mPk.narrowPeak |
| breast | breast | wgEncodeOpenChromDnaseT47dPk.narrowPeak |
| breast | breast | wgEncodeUwDnaseHmecPkRep1.narrowPeak |
| breast | breast | wgEncodeUwDnaseHmecPkRep2.narrowPeak |
| breast | breast | wgEncodeUwDnaseMcf7Est100nm1hPkRep1.narrowPeak |
| breast | breast | wgEncodeUwDnaseMcf7Est100nm1hPkRep2.narrowPeak |
| breast | breast | wgEncodeUwDnaseMcf7Estctrl0hPkRep1.narrowPeak |
| breast | breast | wgEncodeUwDnaseMcf7Estctrl0hPkRep2.narrowPeak |
| breast | breast | wgEncodeUwDnaseMcf7PkRep1.narrowPeak |
| breast | breast | wgEncodeUwDnaseMcf7PkRep2.narrowPeak |
| breast | breast | wgEncodeUwDnaseT47dPkRep1.narrowPeak |
| breast | breast | wgEncodeUwDnaseT47dPkRep2.narrowPeak |
| breast | mammary | wgEncodeAwgDnaseUwHmfUniPk.narrowPeak |
| breast | mammary | wgEncodeUwDnaseHmfPkRep1.narrowPeak |
| breast | mammary | wgEncodeUwDnaseHmfPkRep2.narrowPeak |
| cerebellar | cerebellar | wgEncodeAwgDnaseUwHacUniPk.narrowPeak |
| cerebellar | cerebellar | wgEncodeUwDnaseHacPkRep1.narrowPeak |
| cerebellar | cerebellar | wgEncodeUwDnaseHacPkRep2.narrowPeak |
| cerebellar | cerebellum | wgEncodeOpenChromDnaseCerebellumocPk.narrowPeak |
| cervix | cervix | wgEncodeAwgDnaseDukeHelas3ifna4hUniPk.narrowPeak |
| cervix | cervix | wgEncodeAwgDnaseUwdukeHelas3UniPk.narrowPeak |
| cervix | cervix | wgEncodeOpenChromDnaseHelas3Ifna4hPk.narrowPeak |
| cervix | cervix | wgEncodeOpenChromDnaseHelas3Pk.narrowPeak |
| cervix | cervix | wgEncodeUwDnaseHelas3PkRep1.narrowPeak |
| cervix | cervix | wgEncodeUwDnaseHelas3PkRep2.narrowPeak |
| colon | colon | wgEncodeAwgDnaseUwCaco2UniPk.narrowPeak |
| colon | colon | wgEncodeAwgDnaseUwHct116UniPk.narrowPeak |
| colon | colon | wgEncodeUwDnaseCaco2PkRep1.narrowPeak |
| colon | colon | wgEncodeUwDnaseCaco2PkRep2.narrowPeak |
| colon | colon | wgEncodeUwDnaseHct116PkRep1.narrowPeak |

Enrichment of GWAS variants in epigenomic features

| | | |
|---------------------|----------------------|--|
| colon | colon | wgEncodeUwDnaseHct116PkRep2.narrowPeak |
| connective | connective | wgEncodeAwgDnaseUwHvmfUniPk.narrowPeak |
| connective | connective | wgEncodeUwDnaseHvmfPkRep1.narrowPeak |
| connective | connective | wgEncodeUwDnaseHvmfPkRep2.narrowPeak |
| embryonic_lung | embryonic_lung | wgEncodeAwgDnaseUwWi38tamoxifentamoxifenUniPk.narrowPeak |
| embryonic_lung | embryonic_lung | wgEncodeAwgDnaseUwWi38UniPk.narrowPeak |
| embryonic_lung | embryonic_lung | wgEncodeUwDnaseWi38OhtamPkRep1.narrowPeak |
| embryonic_lung | embryonic_lung | wgEncodeUwDnaseWi38OhtamPkRep2.narrowPeak |
| embryonic_lung | embryonic_lung | wgEncodeUwDnaseWi38PkRep1.narrowPeak |
| embryonic_lung | embryonic_lung | wgEncodeUwDnaseWi38PkRep2.narrowPeak |
| embryonic_stem_cell | embryonic_stem_cell | wgEncodeAwgDnaseDukeH9esUniPk.narrowPeak |
| embryonic_stem_cell | embryonic_stem_cell | wgEncodeAwgDnaseUwdukeH1hescUniPk.narrowPeak |
| embryonic_stem_cell | embryonic_stem_cell | wgEncodeAwgDnaseUwH7hescUniPk.narrowPeak |
| embryonic_stem_cell | embryonic_stem_cell | wgEncodeOpenChromDnaseH1hescPk.narrowPeak |
| embryonic_stem_cell | embryonic_stem_cell | wgEncodeOpenChromDnaseH7esPk.narrowPeak |
| embryonic_stem_cell | embryonic_stem_cell | wgEncodeOpenChromDnaseH9esPk.narrowPeak |
| embryonic_stem_cell | embryonic_stem_cell | wgEncodeUwDnaseH1hescPkRep1.narrowPeak |
| embryonic_stem_cell | embryonic_stem_cell | wgEncodeUwDnaseH7esDiffa14dPkRep1.narrowPeak |
| embryonic_stem_cell | embryonic_stem_cell | wgEncodeUwDnaseH7esDiffa14dPkRep2.narrowPeak |
| embryonic_stem_cell | embryonic_stem_cell | wgEncodeUwDnaseH7esDiffa2dPkRep1.narrowPeak |
| embryonic_stem_cell | embryonic_stem_cell | wgEncodeUwDnaseH7esDiffa5dPkRep1.narrowPeak |
| embryonic_stem_cell | embryonic_stem_cell | wgEncodeUwDnaseH7esDiffa5dPkRep2.narrowPeak |
| embryonic_stem_cell | embryonic_stem_cell | wgEncodeUwDnaseH7esDiffa9dPkRep1.narrowPeak |
| embryonic_stem_cell | embryonic_stem_cell | wgEncodeUwDnaseH7esPkRep1V2.narrowPeak |
| embryonic_stem_cell | embryonic_stem_cell | wgEncodeUwDnaseH7esPkRep2.narrowPeak |
| epithelium | bronchial_epithelium | wgEncodeUwDnaseNhberaPkRep1.narrowPeak |
| epithelium | bronchial_epithelium | wgEncodeUwDnaseNhberaPkRep2.narrowPeak |
| epithelium | epithelium | wgEncodeAwgDnaseDukePhteUniPk.narrowPeak |
| epithelium | epithelium | wgEncodeAwgDnaseUwdukeA549UniPk.narrowPeak |
| epithelium | epithelium | wgEncodeAwgDnaseUwHaepicUniPk.narrowPeak |
| epithelium | epithelium | wgEncodeAwgDnaseUwHcepelicUniPk.narrowPeak |
| epithelium | epithelium | wgEncodeAwgDnaseUwHeepicUniPk.narrowPeak |
| epithelium | epithelium | wgEncodeAwgDnaseUwHipecicUniPk.narrowPeak |

Enrichment of GWAS variants in epigenomic features

| | | |
|------------|------------|--|
| epithelium | epithelium | wgEncodeAwgDnaseUwHnpcepicUniPk.narrowPeak |
| epithelium | epithelium | wgEncodeAwgDnaseUwHpdlfUniPk.narrowPeak |
| epithelium | epithelium | wgEncodeAwgDnaseUwHrcopicUniPk.narrowPeak |
| epithelium | epithelium | wgEncodeAwgDnaseUwHreUniPk.narrowPeak |
| epithelium | epithelium | wgEncodeAwgDnaseUwHrpepicUniPk.narrowPeak |
| epithelium | epithelium | wgEncodeAwgDnaseUwRptecUniPk.narrowPeak |
| epithelium | epithelium | wgEncodeAwgDnaseUwSaecUniPk.narrowPeak |
| epithelium | epithelium | wgEncodeOpenChromDnaseA549Pk.narrowPeak |
| epithelium | epithelium | wgEncodeOpenChromDnasePhtePk.narrowPeak |
| epithelium | epithelium | wgEncodeUwDnaseA549PkRep1.narrowPeak |
| epithelium | epithelium | wgEncodeUwDnaseA549PkRep2.narrowPeak |
| epithelium | epithelium | wgEncodeUwDnaseHaePkRep1.narrowPeak |
| epithelium | epithelium | wgEncodeUwDnaseHaePkRep2.narrowPeak |
| epithelium | epithelium | wgEncodeUwDnaseHcpePkRep1.narrowPeak |
| epithelium | epithelium | wgEncodeUwDnaseHcpePkRep2.narrowPeak |
| epithelium | epithelium | wgEncodeUwDnaseHeePkRep1.narrowPeak |
| epithelium | epithelium | wgEncodeUwDnaseHeePkRep2.narrowPeak |
| epithelium | epithelium | wgEncodeUwDnaseHipePkRep1.narrowPeak |
| epithelium | epithelium | wgEncodeUwDnaseHipePkRep2.narrowPeak |
| epithelium | epithelium | wgEncodeUwDnaseHnpcePkRep1.narrowPeak |
| epithelium | epithelium | wgEncodeUwDnaseHnpcePkRep2V2.narrowPeak |
| epithelium | epithelium | wgEncodeUwDnaseHpdlfPkRep1.narrowPeak |
| epithelium | epithelium | wgEncodeUwDnaseHpdlfPkRep2.narrowPeak |
| epithelium | epithelium | wgEncodeUwDnaseHrccePkRep1.narrowPeak |
| epithelium | epithelium | wgEncodeUwDnaseHrccePkRep2.narrowPeak |
| epithelium | epithelium | wgEncodeUwDnaseHrePkRep1V2.narrowPeak |
| epithelium | epithelium | wgEncodeUwDnaseHrePkRep2V2.narrowPeak |
| epithelium | epithelium | wgEncodeUwDnaseHrpePkRep1V2.narrowPeak |
| epithelium | epithelium | wgEncodeUwDnaseHrpePkRep2V2.narrowPeak |
| epithelium | epithelium | wgEncodeUwDnaseRptecPkRep1.narrowPeak |
| epithelium | epithelium | wgEncodeUwDnaseRptecPkRep2.narrowPeak |
| epithelium | epithelium | wgEncodeUwDnaseSaecPkRep1.narrowPeak |
| epithelium | epithelium | wgEncodeUwDnaseSaecPkRep2.narrowPeak |

Enrichment of GWAS variants in epigenomic features

| | | |
|------------------|--------------------|--|
| epithelium | luminal_epithelium | wgEncodeOpenChromDnaseEcc1Dm002p1hPk.narrowPeak |
| epithelium | luminal_epithelium | wgEncodeOpenChromDnaseEcc1Est10nm30mPk.narrowPeak |
| epithelium | pancreatic_duct | wgEncodeAwgDnaseDukeHpde6e6e7UniPk.narrowPeak |
| epithelium | pancreatic_duct | wgEncodeOpenChromDnaseHpde6e6e7Pk.narrowPeak |
| eye | eye | wgEncodeAwgDnaseUwHconfUniPk.narrowPeak |
| eye | eye | wgEncodeAwgDnaseUwWerirb1UniPk.narrowPeak |
| eye | eye | wgEncodeUwDnaseHconfPkRep1.narrowPeak |
| eye | eye | wgEncodeUwDnaseHconfPkRep2.narrowPeak |
| eye | eye | wgEncodeUwDnaseWerirb1PkRep1.narrowPeak |
| eye | eye | wgEncodeUwDnaseWerirb1PkRep2.narrowPeak |
| fetal_membrane | fetal_membrane | wgEncodeAwgDnaseDukeChorionUniPk.narrowPeak |
| fetal_membrane | fetal_membrane | wgEncodeOpenChromDnaseChorionPk.narrowPeak |
| fibroblasts | lung_fibroblast | wgEncodeOpenChromDnaseFibropag08396Pk.narrowPeak |
| fibroblasts | skin | wgEncodeAwgDnaseDukeFibroblUniPk.narrowPeak |
| fibroblasts | skin | wgEncodeAwgDnaseDukeFibropUniPk.narrowPeak |
| fibroblasts | skin | wgEncodeOpenChromDnaseFibroblgm03348LenticonPk.narrowPeak |
| fibroblasts | skin | wgEncodeOpenChromDnaseFibroblgm03348LentimyodPk.narrowPeak |
| fibroblasts | skin | wgEncodeOpenChromDnaseFibroblgm03348Pk.narrowPeak |
| fibroblasts | skin | wgEncodeOpenChromDnaseFibroblPk.narrowPeak |
| fibroblasts | skin | wgEncodeOpenChromDnaseFibropPk.narrowPeak |
| fibroblasts | skin_fibroblast | wgEncodeOpenChromDnaseFibropag08395Pk.narrowPeak |
| fibroblasts | skin_fibroblast | wgEncodeOpenChromDnaseFibropag20443Pk.narrowPeak |
| foreskin | foreskin | wgEncodeAwgDnaseUwHffmycUniPk.narrowPeak |
| foreskin | foreskin | wgEncodeAwgDnaseUwHffUniPk.narrowPeak |
| foreskin | foreskin | wgEncodeUwDnaseHffmycPkRep1.narrowPeak |
| foreskin | foreskin | wgEncodeUwDnaseHffmycPkRep2.narrowPeak |
| foreskin | foreskin | wgEncodeUwDnaseHffPkRep1.narrowPeak |
| foreskin | foreskin | wgEncodeUwDnaseHffPkRep2.narrowPeak |
| frontal_cerebrum | frontal_cerebrum | wgEncodeOpenChromDnaseCerebrumfrontalocPk.narrowPeak |
| frontal_cortex | frontal_cortex | wgEncodeOpenChromDnaseFrontalcortexocPk.narrowPeak |
| gingival | gingiva | wgEncodeAwgDnaseUwHgfUniPk.narrowPeak |
| gingival | gingiva | wgEncodeUwDnaseHgfPkRep1.narrowPeak |
| gingival | gingiva | wgEncodeUwDnaseHgfPkRep2.narrowPeak |

Enrichment of GWAS variants in epigenomic features

| | | |
|----------|-------------------------------|---|
| gingival | gingival | wgEncodeAwgDnaseUwAg09319UniPk.narrowPeak |
| gingival | gingival | wgEncodeUwDnaseAg09319PkRep1V2.narrowPeak |
| gingival | gingival | wgEncodeUwDnaseAg09319PkRep2.narrowPeak |
| heart | heart | wgEncodeAwgDnaseUwHcfaaUniPk.narrowPeak |
| heart | heart | wgEncodeAwgDnaseUwHcfUniPk.narrowPeak |
| heart | heart | wgEncodeAwgDnaseUwHcmUniPk.narrowPeak |
| heart | heart | wgEncodeOpenChromDnaseHeartocPk.narrowPeak |
| heart | heart | wgEncodeUwDnaseHcfaaPkRep1.narrowPeak |
| heart | heart | wgEncodeUwDnaseHcfaaPkRep2.narrowPeak |
| heart | heart | wgEncodeUwDnaseHcfPkRep1.narrowPeak |
| heart | heart | wgEncodeUwDnaseHcfPkRep2.narrowPeak |
| heart | heart | wgEncodeUwDnaseHcmPkRep1.narrowPeak |
| heart | heart | wgEncodeUwDnaseHcmPkRep2.narrowPeak |
| IPS | induced_pluripotent_cell_iPS | wgEncodeOpenChromDnaselpscwru1Pk.narrowPeak |
| IPS | induced_pluripotent_cell_iPS | wgEncodeOpenChromDnaselpsnih11Pk.narrowPeak |
| IPS | induced_pluripotent_cell_iPS | wgEncodeOpenChromDnaselpsnih7Pk.narrowPeak |
| IPS | induced_pluripotent_stem_cell | wgEncodeAwgDnaseDukelpsUniPk.narrowPeak |
| IPS | induced_pluripotent_stem_cell | wgEncodeOpenChromDnaselpsPk.narrowPeak |
| kidney | kidney | wgEncodeAwgDnaseUwHrgecUniPk.narrowPeak |
| kidney | kidney | wgEncodeOpenChromDnaseHek293tPk.narrowPeak |
| kidney | kidney | wgEncodeUwDnaseHrgecPkRep1.narrowPeak |
| kidney | kidney | wgEncodeUwDnaseHrgecPkRep2.narrowPeak |
| liver | liver | wgEncodeAwgDnaseDuke8988tUniPk.narrowPeak |
| liver | liver | wgEncodeAwgDnaseDukeHepatocytesUniPk.narrowPeak |
| liver | liver | wgEncodeAwgDnaseDukeHuh75UniPk.narrowPeak |
| liver | liver | wgEncodeAwgDnaseDukeHuh7UniPk.narrowPeak |
| liver | liver | wgEncodeAwgDnaseDukeStellateUniPk.narrowPeak |
| liver | liver | wgEncodeAwgDnaseUwdukeHepg2UniPk.narrowPeak |
| liver | liver | wgEncodeOpenChromDnase8988tPk.narrowPeak |
| liver | liver | wgEncodeOpenChromDnaseHepatocytesPk.narrowPeak |
| liver | liver | wgEncodeOpenChromDnaseHepg2Pk.narrowPeak |
| liver | liver | wgEncodeOpenChromDnaseHuh75Pk.narrowPeak |
| liver | liver | wgEncodeOpenChromDnaseHuh7Pk.narrowPeak |

Enrichment of GWAS variants in epigenomic features

| | | |
|--------------|---|--|
| liver | liver | wgEncodeOpenChromDnaseStellatePk.narrowPeak |
| liver | liver | wgEncodeUwDnaseHepg2PkRep1.narrowPeak |
| liver | liver | wgEncodeUwDnaseHepg2PkRep2.narrowPeak |
| lung | lung | wgEncodeAwgDnaseUwAg04450UniPk.narrowPeak |
| lung | lung | wgEncodeAwgDnaseUwHpfUniPk.narrowPeak |
| lung | lung | wgEncodeAwgDnaseUwNhlfUniPk.narrowPeak |
| lung | lung | wgEncodeOpenChromDnaselmr90Pk.narrowPeak |
| lung | lung | wgEncodeUwDnaseAg04450PkRep1.narrowPeak |
| lung | lung | wgEncodeUwDnaseAg04450PkRep2.narrowPeak |
| lung | lung | wgEncodeUwDnaseHpfPkRep1.narrowPeak |
| lung | lung | wgEncodeUwDnaseHpfPkRep2.narrowPeak |
| lung | lung | wgEncodeUwDnaseNhlfPkRep1.narrowPeak |
| lung | lung | wgEncodeUwDnaseNhlfPkRep2.narrowPeak |
| melanoma | Melanoma_cell_line_derived_from_melanoma_metastasis | wgEncodeOpenChromDnaseMe12183Pk.narrowPeak |
| monocytes | monocytes | wgEncodeAwgDnaseUwMonocytescd14ro01746UniPk.narrowPeak |
| monocytes | monocytes | wgEncodeOpenChromDnaseMonocd14Pk.narrowPeak |
| monocytes | monocytes | wgEncodeUwDnaseMonocd14ro1746PkRep2.narrowPeak |
| muscle | muscle | wgEncodeAwgDnaseDukeHsmmembUniPk.narrowPeak |
| muscle | muscle | wgEncodeAwgDnaseUwdukeHsmmtubeUniPk.narrowPeak |
| muscle | muscle | wgEncodeAwgDnaseUwSkmcUniPk.narrowPeak |
| muscle | muscle | wgEncodeOpenChromDnaseHsmmembPk.narrowPeak |
| muscle | muscle | wgEncodeOpenChromDnaseHsmmfshdPk.narrowPeak |
| muscle | muscle | wgEncodeOpenChromDnaseHsmmtPk.narrowPeak |
| muscle | muscle | wgEncodeUwDnaseHsmmtPkRep1.narrowPeak |
| muscle | muscle | wgEncodeUwDnaseHsmmtPkRep2.narrowPeak |
| muscle | muscle | wgEncodeUwDnaseSkmcPkRep1.narrowPeak |
| muscle | muscle | wgEncodeUwDnaseSkmcPkRep2.narrowPeak |
| muscle | psoas_muscle | wgEncodeOpenChromDnasePsoasmuscleoPk.narrowPeak |
| myometrium | myometrium | wgEncodeAwgDnaseDukeMyometrUniPk.narrowPeak |
| myometrium | myometrium | wgEncodeOpenChromDnaseMyometrPk.narrowPeak |
| nasal_biopsy | nasal_biopsy | wgEncodeOpenChromDnaseOlfneurospherePk.narrowPeak |
| pancreas | pancreas | wgEncodeAwgDnaseDukePanisletdUniPk.narrowPeak |
| pancreas | pancreas | wgEncodeAwgDnaseDukePanisletsUniPk.narrowPeak |

Enrichment of GWAS variants in epigenomic features

| | | |
|--------------------------|--------------------------|---|
| pancreas | pancreas | wgEncodeAwgDnaseUwPanc1UniPk.narrowPeak |
| pancreas | pancreas | wgEncodeOpenChromDnasePanisdPk.narrowPeak |
| pancreas | pancreas | wgEncodeOpenChromDnasePanisletsPk.narrowPeak |
| pancreas | pancreas | wgEncodeUwDnasePanc1PkRep1.narrowPeak |
| pancreas | pancreas | wgEncodeUwDnasePanc1PkRep2.narrowPeak |
| prostate | prostate | wgEncodeAwgDnaseDukeLncapandrogenUniPk.narrowPeak |
| prostate | prostate | wgEncodeAwgDnaseDukeRwpe1UniPk.narrowPeak |
| prostate | prostate | wgEncodeAwgDnaseUwdukeLncapUniPk.narrowPeak |
| prostate | prostate | wgEncodeAwgDnaseUwPrecUniPk.narrowPeak |
| prostate | prostate | wgEncodeOpenChromDnaseLncapAndroPk.narrowPeak |
| prostate | prostate | wgEncodeOpenChromDnaseLncapPk.narrowPeak |
| prostate | prostate | wgEncodeOpenChromDnaseRwpe1Pk.narrowPeak |
| prostate | prostate | wgEncodeUwDnaseLncapPkRep1.narrowPeak |
| prostate | prostate | wgEncodeUwDnaseLncapPkRep2.narrowPeak |
| prostate | prostate | wgEncodeUwDnasePrecPkRep1.narrowPeak |
| prostate | prostate | wgEncodeUwDnasePrecPkRep2.narrowPeak |
| skeletal_muscle_myoblast | skeletal_muscle_myoblast | wgEncodeAwgDnaseUwdukeHsmmUniPk.narrowPeak |
| skeletal_muscle_myoblast | skeletal_muscle_myoblast | wgEncodeOpenChromDnaseHsmmPk.narrowPeak |
| skeletal_muscle_myoblast | skeletal_muscle_myoblast | wgEncodeUwDnaseHsmmPkRep1.narrowPeak |
| skeletal_muscle_myoblast | skeletal_muscle_myoblast | wgEncodeUwDnaseHsmmPkRep2.narrowPeak |
| skeletal_muscle_myoblast | skeletal_muscle_myoblast | wgEncodeUwDnaseLhcnm2Diff4dPkRep1.narrowPeak |
| skeletal_muscle_myoblast | skeletal_muscle_myoblast | wgEncodeUwDnaseLhcnm2Diff4dPkRep2.narrowPeak |
| skeletal_muscle_myoblast | skeletal_muscle_myoblast | wgEncodeUwDnaseLhcnm2PkRep1.narrowPeak |
| skeletal_muscle_myoblast | skeletal_muscle_myoblast | wgEncodeUwDnaseLhcnm2PkRep2.narrowPeak |
| skin | skin | wgEncodeAwgDnaseDukeMelanoUniPk.narrowPeak |
| skin | skin | wgEncodeAwgDnaseDukeProgfibUniPk.narrowPeak |
| skin | skin | wgEncodeAwgDnaseUwAg04449UniPk.narrowPeak |
| skin | skin | wgEncodeAwgDnaseUwAg09309UniPk.narrowPeak |
| skin | skin | wgEncodeAwgDnaseUwAg10803UniPk.narrowPeak |
| skin | skin | wgEncodeAwgDnaseUwBjUniPk.narrowPeak |
| skin | skin | wgEncodeAwgDnaseUwdukeNhekUniPk.narrowPeak |
| skin | skin | wgEncodeAwgDnaseUwNhdfadUniPk.narrowPeak |
| skin | skin | wgEncodeAwgDnaseUwNhdfneoUniPk.narrowPeak |

Enrichment of GWAS variants in epigenomic features

| | | |
|-------------|-------------|---|
| skin | skin | wgEncodeOpenChromDnaseColo829Pk.narrowPeak |
| skin | skin | wgEncodeOpenChromDnaseMelanoPk.narrowPeak |
| skin | skin | wgEncodeOpenChromDnaseNhekPk.narrowPeak |
| skin | skin | wgEncodeOpenChromDnaseProgfibPk.narrowPeak |
| skin | skin | wgEncodeUwDnaseAg04449PkRep1.narrowPeak |
| skin | skin | wgEncodeUwDnaseAg04449PkRep2.narrowPeak |
| skin | skin | wgEncodeUwDnaseAg09309PkRep1.narrowPeak |
| skin | skin | wgEncodeUwDnaseAg09309PkRep2.narrowPeak |
| skin | skin | wgEncodeUwDnaseAg10803PkRep1.narrowPeak |
| skin | skin | wgEncodeUwDnaseAg10803PkRep2.narrowPeak |
| skin | skin | wgEncodeUwDnaseBjPkRep1.narrowPeak |
| skin | skin | wgEncodeUwDnaseBjPkRep2.narrowPeak |
| skin | skin | wgEncodeUwDnaseGm04503PkRep1.narrowPeak |
| skin | skin | wgEncodeUwDnaseGm04503PkRep2.narrowPeak |
| skin | skin | wgEncodeUwDnaseGm04504PkRep1.narrowPeak |
| skin | skin | wgEncodeUwDnaseGm04504PkRep2.narrowPeak |
| skin | skin | wgEncodeUwDnaseNhdfadPkRep1.narrowPeak |
| skin | skin | wgEncodeUwDnaseNhdfadPkRep2.narrowPeak |
| skin | skin | wgEncodeUwDnaseNhdfneoPkRep1.narrowPeak |
| skin | skin | wgEncodeUwDnaseNhdfneoPkRep2.narrowPeak |
| skin | skin | wgEncodeUwDnaseNhekPkRep1.narrowPeak |
| skin | skin | wgEncodeUwDnaseNhekPkRep2.narrowPeak |
| skin | skin | wgEncodeUwDnaseRpmi7951PkRep1.narrowPeak |
| skin | skin | wgEncodeUwDnaseRpmi7951PkRep2.narrowPeak |
| spinal_cord | spinal_cord | wgEncodeAwgDnaseUwHaspUniPk.narrowPeak |
| spinal_cord | spinal_cord | wgEncodeUwDnaseHaspPkRep1.narrowPeak |
| spinal_cord | spinal_cord | wgEncodeUwDnaseHaspPkRep2.narrowPeak |
| testis | testis | wgEncodeAwgDnaseUwNt2d1UniPk.narrowPeak |
| testis | testis | wgEncodeUwDnaseNt2d1PkRep1.narrowPeak |
| testis | testis | wgEncodeUwDnaseNt2d1PkRep2.narrowPeak |
| tonsil | tonsil | wgEncodeOpenChromDnaseGcbcellPk.narrowPeak |
| tonsil | tonsil | wgEncodeOpenChromDnaseNaivebcellPk.narrowPeak |
| urothelium | urothelium | wgEncodeAwgDnaseDukeUrotheliaUniPk.narrowPeak |

Enrichment of GWAS variants in epigenomic features

| | | |
|------------|------------|---|
| urothelium | urothelium | wgEncodeAwgDnaseDukeUrotheliaut189UniPk.narrowPeak |
| urothelium | urothelium | wgEncodeOpenChromDnaseUrothePkV2.narrowPeak |
| urothelium | urothelium | wgEncodeOpenChromDnaseUrotheUt189PkV2.narrowPeak |
| uterus | uterus | wgEncodeAwgDnaseDukeLshikawaestradiolUniPk.narrowPeak |
| uterus | uterus | wgEncodeAwgDnaseDukeLshikawatamoxifenUniPk.narrowPeak |
| uterus | uterus | wgEncodeOpenChromDnaseLshikawaEst10nm30mPk.narrowPeak |
| uterus | uterus | wgEncodeOpenChromDnaseLshikawaTam10030Pk.narrowPeak |

Supplementary Table 2. Enrichment of GWAS loci in DNase hypersensitive sites of common tissues.

A. Body Mass Index (BMI) and Blood Pressure (BP)

| Bed_File | BMI_InBed_Index_SNP | BMI_ExpectNum_of_InBed_SNP | BMI_PValue | BP_InBed_Index_SNP | BP_ExpectNum_of_InBed_SNP | BP_PValue |
|--------------------------|---------------------|----------------------------|------------|--------------------|---------------------------|-----------|
| heart | 57 | 41.24 | 0.00029 | 64 | 39.56 | 0.00000 |
| blood | 64 | 60.63 | 0.25540 | 77 | 60.99 | 0.00016 |
| liver | 61 | 47.73 | 0.00250 | 64 | 48.20 | 0.00043 |
| skin | 69 | 59.97 | 0.02090 | 76 | 57.94 | 0.00002 |
| IPS | 52 | 38.09 | 0.00140 | 54 | 37.47 | 0.00023 |
| blood_vessel | 63 | 53.30 | 0.01750 | 78 | 51.61 | 0.00000 |
| bone | 49 | 37.55 | 0.00675 | 54 | 36.15 | 0.00007 |
| frontal_cortex | 39 | 22.99 | 0.00009 | 43 | 22.73 | 0.00000 |
| fibroblasts | 60 | 50.25 | 0.01857 | 66 | 49.20 | 0.00014 |
| nasal_biopsy | 40 | 23.46 | 0.00004 | 41 | 22.50 | 0.00001 |
| breast | 77 | 61.57 | 0.00014 | 75 | 60.98 | 0.00064 |
| epithelium | 70 | 63.04 | 0.05891 | 76 | 61.43 | 0.00035 |
| muscle | 66 | 49.82 | 0.00020 | 69 | 48.87 | 0.00001 |
| skeletal_muscle_myoblast | 60 | 44.95 | 0.00054 | 63 | 43.32 | 0.00001 |
| myometrium | 39 | 30.22 | 0.02555 | 49 | 29.35 | 0.00001 |
| frontal_cerebrum | 36 | 24.85 | 0.00503 | 42 | 24.83 | 0.00005 |
| prostate | 66 | 51.51 | 0.00071 | 66 | 49.48 | 0.00016 |

Enrichment of GWAS variants in epigenomic features

| | | | | | | | |
|---------------------|----|-------|---------|----|--|-------|---------|
| pancreas | 55 | 42.27 | 0.00320 | 58 | | 41.66 | 0.00025 |
| fetal_membrane | 43 | 28.17 | 0.00046 | 44 | | 27.82 | 0.00020 |
| monocytes | 43 | 29.60 | 0.00152 | 44 | | 29.24 | 0.00067 |
| brain | 75 | 60.89 | 0.00052 | 82 | | 59.12 | 0.00000 |
| cervix | 53 | 37.42 | 0.00036 | 55 | | 36.59 | 0.00004 |
| connective | 27 | 24.50 | 0.30142 | 38 | | 22.95 | 0.00015 |
| gingival | 33 | 25.31 | 0.03684 | 39 | | 23.75 | 0.00014 |
| tonsil | 35 | 24.54 | 0.00678 | 36 | | 23.44 | 0.00164 |
| colon | 39 | 28.52 | 0.00806 | 40 | | 26.45 | 0.00090 |
| embryonic_stem_cell | 67 | 57.77 | 0.02050 | 73 | | 55.59 | 0.00005 |
| cerebellar | 50 | 36.12 | 0.00117 | 56 | | 34.90 | 0.00000 |
| melanoma | 36 | 28.61 | 0.04666 | 32 | | 27.03 | 0.13065 |
| uterus | 40 | 31.93 | 0.03721 | 40 | | 29.81 | 0.01095 |
| urothelium | 43 | 33.81 | 0.02256 | 45 | | 32.98 | 0.00416 |
| kidney | 45 | 33.92 | 0.00685 | 50 | | 32.54 | 0.00005 |
| lung | 56 | 41.66 | 0.00091 | 59 | | 39.68 | 0.00002 |
| embryonic_lung | 37 | 28.69 | 0.03081 | 41 | | 26.96 | 0.00063 |
| foreskin | 40 | 31.28 | 0.02568 | 47 | | 29.19 | 0.00002 |
| blastula | 34 | 26.40 | 0.04143 | 39 | | 25.28 | 0.00078 |
| bone_marrow | 47 | 36.11 | 0.00757 | 49 | | 33.81 | 0.00029 |
| spinal_cord | 42 | 29.09 | 0.00139 | 33 | | 25.73 | 0.04523 |
| brain_hippocampus | 39 | 28.45 | 0.00756 | 33 | | 25.83 | 0.04771 |
| testis | 32 | 28.13 | 0.19746 | 36 | | 25.21 | 0.00509 |
| eye | 44 | 36.98 | 0.06586 | 46 | | 34.49 | 0.00524 |

B. Coronary Artery Disease (CAD), Lipids, and Type 2 Diabetes (T2D)

| Bed_File | CAD_InBed_Index_SNP | CAD_ExpectNum_of_InBed_SNP | CAD_PValue | lipids_InBed_Index_SNP | lipids_ExpectNum_of_InBed_SNP | lipids_PValue | T2D_InBed_Index_SNP | T2D_ExpectNum_of_InBed_SNP | T2D_PValue |
|----------|---------------------|----------------------------|------------|------------------------|-------------------------------|---------------|---------------------|----------------------------|------------|
| heart | 28 | 16.32 | 0.00002 | 90 | 65.14 | 0.00001 | 43 | 24.95 | 0.00000 |

Enrichment of GWAS variants in epigenomic features

| | | | | | | | | | |
|--------------------------|----|-------|---------|-----|-------|---------|----|-------|---------|
| blood | 34 | 24.34 | 0.00006 | 133 | 98.38 | 0.00000 | 53 | 39.54 | 0.00014 |
| liver | 30 | 19.52 | 0.00012 | 121 | 77.57 | 0.00000 | 48 | 30.88 | 0.00001 |
| skin | 33 | 23.78 | 0.00013 | 116 | 94.69 | 0.00004 | 45 | 38.10 | 0.03792 |
| IPS | 25 | 15.18 | 0.00046 | 83 | 60.19 | 0.00005 | 33 | 23.20 | 0.00664 |
| blood_vessel | 30 | 20.93 | 0.00050 | 98 | 84.28 | 0.00844 | 47 | 32.67 | 0.00009 |
| bone | 24 | 14.61 | 0.00083 | 85 | 58.75 | 0.00000 | 37 | 22.80 | 0.00013 |
| frontal_cortex | 18 | 9.23 | 0.00084 | 71 | 37.41 | 0.00000 | 25 | 14.21 | 0.00119 |
| fibroblasts | 29 | 20.08 | 0.00089 | 111 | 79.99 | 0.00000 | 46 | 31.74 | 0.00010 |
| nasal_biopsy | 18 | 9.67 | 0.00134 | 58 | 37.15 | 0.00004 | 24 | 14.05 | 0.00207 |
| breast | 32 | 24.48 | 0.00170 | 122 | 98.18 | 0.00000 | 52 | 39.21 | 0.00025 |
| epithelium | 32 | 24.69 | 0.00210 | 119 | 99.73 | 0.00013 | 54 | 40.19 | 0.00005 |
| muscle | 28 | 19.90 | 0.00249 | 108 | 79.38 | 0.00000 | 46 | 30.98 | 0.00006 |
| skeletal_muscle_myoblast | 26 | 18.04 | 0.00312 | 93 | 71.36 | 0.00009 | 42 | 27.79 | 0.00012 |
| myometrium | 20 | 12.12 | 0.00338 | 68 | 48.54 | 0.00024 | 26 | 18.39 | 0.02075 |
| frontal_cerebrum | 18 | 10.26 | 0.00360 | 76 | 40.51 | 0.00000 | 24 | 15.41 | 0.00901 |
| prostate | 28 | 20.44 | 0.00392 | 107 | 81.16 | 0.00000 | 45 | 32.05 | 0.00041 |
| pancreas | 25 | 17.20 | 0.00431 | 92 | 68.16 | 0.00002 | 41 | 26.45 | 0.00010 |
| fetal_membrane | 19 | 11.47 | 0.00518 | 74 | 45.85 | 0.00000 | 32 | 17.70 | 0.00007 |
| monocytes | 19 | 11.74 | 0.00726 | 89 | 48.04 | 0.00000 | 33 | 18.16 | 0.00004 |
| brain | 30 | 23.82 | 0.01197 | 109 | 95.87 | 0.00945 | 53 | 38.38 | 0.00003 |
| cervix | 22 | 15.20 | 0.01209 | 81 | 59.09 | 0.00008 | 37 | 23.28 | 0.00021 |
| connective | 16 | 10.01 | 0.01448 | 56 | 38.41 | 0.00038 | 26 | 14.17 | 0.00026 |
| gingival | 16 | 10.05 | 0.01580 | 57 | 39.22 | 0.00034 | 26 | 14.64 | 0.00055 |
| tonsil | 16 | 9.96 | 0.01607 | 70 | 38.62 | 0.00000 | 25 | 14.05 | 0.00090 |
| colon | 17 | 11.25 | 0.02329 | 71 | 44.24 | 0.00000 | 29 | 16.70 | 0.00034 |
| embryonic_stem_cell | 28 | 22.55 | 0.02870 | 107 | 90.35 | 0.00156 | 53 | 36.17 | 0.00000 |
| cerebellar | 20 | 14.64 | 0.03683 | 74 | 58.41 | 0.00304 | 34 | 22.08 | 0.00092 |
| melanoma | 16 | 11.18 | 0.04524 | 64 | 43.98 | 0.00010 | 22 | 16.15 | 0.05325 |
| uterus | 17 | 12.01 | 0.04567 | 72 | 48.91 | 0.00001 | 32 | 18.02 | 0.00008 |
| urothelium | 18 | 13.33 | 0.06275 | 72 | 52.88 | 0.00038 | 31 | 20.44 | 0.00265 |
| kidney | 18 | 13.51 | 0.06817 | 75 | 52.58 | 0.00003 | 31 | 19.78 | 0.00141 |

Enrichment of GWAS variants in epigenomic features

| | | | | | | | | | |
|-------------------|----|-------|---------|----|-------|---------|----|-------|---------|
| lung | 21 | 16.46 | 0.07114 | 89 | 65.70 | 0.00003 | 41 | 25.74 | 0.00004 |
| embryonic_lung | 16 | 11.72 | 0.07310 | 59 | 45.50 | 0.00682 | 30 | 16.83 | 0.00014 |
| foreskin | 17 | 12.81 | 0.08045 | 58 | 48.40 | 0.04169 | 30 | 18.05 | 0.00053 |
| blastula | 14 | 10.73 | 0.14100 | 63 | 41.54 | 0.00004 | 26 | 15.85 | 0.00239 |
| bone_marrow | 17 | 14.13 | 0.18233 | 69 | 55.72 | 0.00796 | 32 | 20.72 | 0.00125 |
| spinal_cord | 13 | 10.96 | 0.26115 | 57 | 44.25 | 0.00797 | 24 | 16.05 | 0.01249 |
| brain_hippocampus | 13 | 11.25 | 0.30365 | 56 | 44.53 | 0.01596 | 32 | 16.00 | 0.00000 |
| testis | 12 | 10.84 | 0.38860 | 54 | 42.32 | 0.01408 | 25 | 15.08 | 0.00225 |
| eye | 14 | 14.41 | 0.63104 | 73 | 57.72 | 0.00318 | 38 | 21.54 | 0.00001 |

Supplementary Table 3. Fold enrichment of lipid loci in DNase hypersensitive sites at different consensus thresholds.

| Bed_File | InBed_Index_SNP_100 | ExpectNum_of_InBed_SNP_100 | PVal_ue_100 | InBed_Index_SNP_75 | ExpectNum_of_InBed_SNP_75 | PVal_ue_75 | InBed_Index_SNP_50 | ExpectNum_of_InBed_SNP_50 | PVal_ue_50 | InBed_Index_SNP_25 | ExpectNum_of_InBed_SNP_25 | PVal_ue_25 | InBed_Index_SNP_uni0n | ExpectNum_of_InBed_SNP_union | PVal_ue_uni0n |
|----------------|---------------------|----------------------------|-------------|--------------------|---------------------------|------------|--------------------|---------------------------|------------|--------------------|---------------------------|------------|-----------------------|------------------------------|---------------|
| blastula | 36 | 21.47 | 0.00053 | 36 | 21.47 | 0.00053 | 63 | 41.54 | 0.00004 | 63 | 41.54 | 0.00004 | 63 | 41.54 | 0.00004 |
| blood | 0 | NA | NA | 16 | 7.99 | 0.00449 | 26 | 15.22 | 0.00301 | 63 | 32.85 | 0.00000 | 133 | 98.38 | 0.00000 |
| blood_vessel | 4 | 2.90 | 0.32853 | 20 | 12.49 | 0.01912 | 31 | 21.50 | 0.01522 | 50 | 34.62 | 0.00118 | 98 | 84.28 | 0.00844 |
| bone | 12 | 6.04 | 0.01578 | 19 | 11.38 | 0.01560 | 38 | 28.47 | 0.02371 | 60 | 46.12 | 0.00525 | 101 | 79.41 | 0.00008 |
| brain | 1 | 1.24 | 0.71722 | 13 | 6.86 | 0.01745 | 20 | 13.32 | 0.03740 | 49 | 35.46 | 0.00396 | 117 | 102.44 | 0.00357 |
| breast | 4 | 2.05 | 0.14653 | 17 | 11.62 | 0.06437 | 34 | 21.90 | 0.00328 | 68 | 44.39 | 0.00001 | 122 | 98.18 | 0.00000 |
| cervix | 14 | 8.43 | 0.03795 | 24 | 14.05 | 0.00458 | 42 | 30.08 | 0.00766 | 63 | 44.89 | 0.00047 | 81 | 59.09 | 0.00008 |
| colon | 9 | 4.79 | 0.04720 | 12 | 6.65 | 0.03071 | 40 | 24.35 | 0.00032 | 59 | 36.51 | 0.00001 | 71 | 44.24 | 0.00000 |
| connective | 42 | 22.90 | 0.00001 | 42 | 22.90 | 0.00001 | 50 | 31.15 | 0.00007 | 56 | 38.41 | 0.000038 | 56 | 38.41 | 0.000038 |
| embryonic_lung | 22 | 14.85 | 0.03232 | 28 | 20.03 | 0.03236 | 38 | 32.38 | 0.13776 | 52 | 41.83 | 0.02941 | 59 | 45.50 | 0.00682 |

Enrichment of GWAS variants in epigenomic features

| | | | | | | | | | | | | | | | |
|--------------------------|----|-------|-------------|----|-------|-------------|----|-------|-------------|----|-------|-------------|-----|--------|-------------|
| embryonic_stem_cell | 7 | 3.97 | 0.09 952 | 20 | 10.54 | 0.00 318 | 39 | 20.84 | 0.00 002 | 56 | 45.67 | 0.03 125 | 107 | 90.35 | 0.001 56 |
| epithelium | 3 | 2.35 | 0.42 011 | 17 | 11.53 | 0.06 084 | 33 | 22.23 | 0.00 718 | 50 | 40.27 | 0.03 171 | 119 | 99.08 | 0.000 08 |
| eye | 12 | 7.29 | 0.05 668 | 15 | 10.10 | 0.07 328 | 56 | 40.22 | 0.00 129 | 68 | 49.47 | 0.00 034 | 73 | 57.72 | 0.003 18 |
| fetal_memb_rane | 35 | 20.40 | 0.00 051 | 35 | 20.40 | 0.00 051 | 74 | 45.85 | 0.00 000 | 74 | 45.85 | 0.00 000 | 74 | 45.85 | 0.000 00 |
| foreskin | 25 | 16.00 | 0.01 219 | 35 | 22.25 | 0.00 214 | 45 | 33.98 | 0.01 447 | 55 | 44.53 | 0.02 679 | 58 | 48.40 | 0.041 69 |
| gingival | 27 | 15.11 | 0.00 126 | 30 | 18.08 | 0.00 213 | 46 | 28.83 | 0.00 019 | 49 | 34.29 | 0.00 185 | 57 | 39.22 | 0.000 34 |
| heart | 9 | 5.85 | 0.12 673 | 24 | 16.79 | 0.03 835 | 45 | 29.99 | 0.00 101 | 54 | 41.39 | 0.00 863 | 90 | 65.14 | 0.000 01 |
| IPS | 35 | 18.44 | 0.00 007 | 52 | 34.02 | 0.00 028 | 64 | 40.82 | 0.00 001 | 71 | 48.13 | 0.00 003 | 83 | 60.19 | 0.000 05 |
| kidney | 13 | 9.39 | 0.13 796 | 31 | 21.48 | 0.01 463 | 44 | 29.15 | 0.00 099 | 75 | 52.58 | 0.00 003 | 75 | 52.58 | 0.000 03 |
| liver | 7 | 2.66 | 0.01 629 | 19 | 8.99 | 0.00 115 | 45 | 22.27 | 0.00 000 | 78 | 38.84 | 0.00 000 | 121 | 77.57 | 0.000 00 |
| lung | 15 | 9.50 | 0.04 747 | 23 | 15.32 | 0.02 571 | 36 | 25.57 | 0.01 241 | 55 | 42.78 | 0.01 123 | 92 | 67.75 | 0.000 01 |
| monocytes | 32 | 15.01 | 0.00 001 | 32 | 15.01 | 0.00 001 | 50 | 24.85 | 0.00 000 | 89 | 48.04 | 0.00 000 | 89 | 48.04 | 0.000 00 |
| muscle | 9 | 5.96 | 0.13 754 | 22 | 12.71 | 0.00 613 | 34 | 26.70 | 0.06 517 | 77 | 56.80 | 0.00 021 | 108 | 79.38 | 0.000 00 |
| myometrium | 37 | 25.52 | 0.00 658 | 37 | 25.52 | 0.00 658 | 68 | 48.54 | 0.00 024 | 68 | 48.54 | 0.00 024 | 68 | 48.54 | 0.000 24 |
| nasal_biopsy | 58 | 37.15 | 0.00 004 | 58 | 37.15 | 0.000 04 |
| pancreas | 4 | 4.55 | 0.67 706 | 18 | 9.82 | 0.00 723 | 25 | 19.16 | 0.08 571 | 55 | 36.06 | 0.00 013 | 100 | 73.80 | 0.000 00 |
| prostate | 6 | 4.85 | 0.35 503 | 11 | 9.19 | 0.30 823 | 30 | 20.29 | 0.01 235 | 74 | 55.50 | 0.00 041 | 107 | 81.16 | 0.000 00 |
| skeletal_muscle_myoblast | 10 | 8.64 | 0.36 178 | 31 | 21.49 | 0.01 585 | 47 | 34.61 | 0.00 760 | 69 | 54.35 | 0.00 446 | 93 | 71.36 | 0.000 09 |
| skin | 1 | 1.99 | 0.87 188 | 19 | 12.46 | 0.03 690 | 32 | 22.94 | 0.02 273 | 56 | 43.06 | 0.00 807 | 126 | 104.57 | 0.000 02 |
| spinal_cord | 22 | 15.67 | 0.05 588 | 22 | 15.67 | 0.05 588 | 43 | 34.25 | 0.04 038 | 57 | 44.25 | 0.00 797 | 57 | 44.25 | 0.007 97 |
| testis | 32 | 22.66 | 0.01 840 | 32 | 22.66 | 0.01 840 | 49 | 36.30 | 0.00 656 | 54 | 42.32 | 0.01 408 | 54 | 42.32 | 0.014 08 |
| tonsil | 54 | 30.03 | 0.00 000 | 54 | 30.03 | 0.00 000 | 70 | 38.62 | 0.00 000 | 70 | 38.62 | 0.00 000 | 70 | 38.62 | 0.000 00 |
| urothelium | 22 | 15.90 | 0.06 498 | 30 | 25.07 | 0.15 255 | 59 | 39.96 | 0.00 021 | 72 | 52.88 | 0.00 038 | 72 | 52.88 | 0.000 38 |
| uterus | 30 | 18.31 | 0.00 261 | 42 | 26.70 | 0.00 057 | 64 | 41.67 | 0.00 002 | 72 | 48.91 | 0.00 001 | 72 | 48.91 | 0.000 01 |

Supplementary Table 4. Enrichment of GWAS loci for five traits or diseases (BMI; Body Mass Index, BP; Blood Pressure, CAD; Coronary Artery Disease, Lipids, T2D; Type 2 Diabetes) in predicted chromatin states.

| Chromatin_State | BMI_InBed_Index_SNP | BMI_ExpectNum_of_InBed_SNP | BMI_PValue | BP_InBed_Index_SNP | BP_ExpectNum_of_InBed_SNP | BP_PValue | CAD_InBed_Index_SNP | CAD_ExpectNum_of_InBed_SNP | CAD_PValue | lipids_InBed_Index_SNP | lipids_ExpectNum_of_InBed_SNP | lipids_PValue | T2D_InBed_Index_SNP | T2D_ExpectNum_of_InBed_SNP | T2D_PValue |
|--|---------------------|----------------------------|------------|--------------------|---------------------------|-----------|---------------------|----------------------------|------------|------------------------|-------------------------------|---------------|---------------------|----------------------------|------------|
| wgEncodeBroadHmmGm12878HMM_10_Txn_Elongation | 28 | 17.42 | 0.00306 | 28 | 16.24 | 0.00119 | 14 | 7.30 | 0.00492 | 60 | 28.73 | 0.00000 | 16 | 9.73 | 0.02299 |
| wgEncodeBroadHmmGm12878HMM_11_Weak_Txn | 41 | 32.44 | 0.03254 | 47 | 31.80 | 0.00060 | 18 | 13.22 | 0.06184 | 86 | 53.30 | 0.00000 | 29 | 20.31 | 0.01284 |
| wgEncodeBroadHmmGm12878HMM_12_Repressed | 25 | 17.34 | 0.02940 | 27 | 17.37 | 0.00935 | 17 | 7.29 | 0.00020 | 38 | 26.86 | 0.01322 | 24 | 10.97 | 0.00006 |
| wgEncodeBroadHmmGm12878HMM_13_Heterochrom | 86 | 88.60 | 0.87378 | 88 | 87.57 | 0.52629 | 29 | 32.34 | 0.97732 | 135 | 140.64 | 0.94552 | 62 | 58.17 | 0.07573 |
| wgEncodeBroadHmmGm12878HMM_14_Repetitive_CNV | 6 | 2.30 | 0.02484 | 3 | 1.92 | 0.30015 | 1 | 0.76 | 0.54277 | 6 | 3.32 | 0.11233 | 3 | 1.04 | 0.08488 |
| wgEncodeBroadHmmGm12878HMM_15_Repetitive_CNV | 5 | 1.55 | 0.01683 | 1 | 1.26 | 0.73663 | 0 | NA | NA | 3 | 1.97 | 0.31591 | 1 | 0.60 | 0.46226 |
| wgEncodeBroadHmmGm12878HMM_1_Active_Promoter | 20 | 12.13 | 0.00978 | 25 | 10.70 | 0.00001 | 6 | 4.68 | 0.31572 | 37 | 18.76 | 0.00001 | 7 | 5.97 | 0.38554 |
| wgEncodeBroadHmmGm12878HMM_2_Weak_Promoter | 16 | 13.08 | 0.21245 | 22 | 11.42 | 0.00082 | 10 | 5.12 | 0.01570 | 34 | 20.25 | 0.000068 | 4 | 6.89 | 0.93479 |
| wgEncodeBroadHmmGm12878HMM_3_Poised_Promoter | 6 | 2.35 | 0.02863 | 3 | 2.43 | 0.44056 | 0 | NA | NA | 6 | 3.86 | 0.18785 | 4 | 1.44 | 0.05248 |
| wgEncodeBroadHmmGm12878HMM_4_Strong_Enhancer | 19 | 10.14 | 0.00367 | 22 | 9.27 | 0.00006 | 8 | 3.92 | 0.03291 | 34 | 15.45 | 0.00000 | 10 | 5.69 | 0.05065 |
| wgEncodeBroadHmmGm12878HMM_5_Strong_Enhancer | 14 | 11.62 | 0.26229 | 22 | 10.22 | 0.00025 | 10 | 4.60 | 0.00857 | 34 | 18.20 | 0.000011 | 6 | 6.09 | 0.58329 |
| wgEncodeBroadHmmGm12878HMM_6_Weak_Enhancer | 24 | 17.82 | 0.05573 | 24 | 16.29 | 0.02094 | 11 | 6.91 | 0.05770 | 48 | 27.74 | 0.00001 | 16 | 9.63 | 0.01943 |
| wgEncodeBroadHmmGm12878HMM_7_Weak_Enhancer | 29 | 24.99 | 0.18870 | 36 | 23.29 | 0.00157 | 11 | 9.82 | 0.38312 | 68 | 38.94 | 0.00000 | 26 | 14.43 | 0.00052 |

Enrichment of GWAS variants in epigenomic features

| | | | | | | | | | | | | | | | |
|--|----|-------|-------------|----|-------|-------------|----|-------|-------------|-----|--------|-------------|----|-------|-------------|
| wgEncodeBroadHmmGm12878HMM_8_Insulator | 20 | 13.90 | 0.04 352 | 9 | 11.55 | 0.84 645 | 8 | 4.89 | 0.09 463 | 29 | 19.59 | 0.013 81 | 7 | 6.69 | 0.51 305 |
| wgEncodeBroadHmmGm12878HMM_9_Txn_Transition | 14 | 8.41 | 0.03 222 | 18 | 7.24 | 0.00 016 | 8 | 3.42 | 0.01 316 | 25 | 13.65 | 0.001 30 | 4 | 4.38 | 0.65 457 |
| wgEncodeBroadHmmH1heschHMM_10_Txn_Elongation | 24 | 12.94 | 0.00 099 | 21 | 12.17 | 0.00 601 | 16 | 5.33 | 0.00 001 | 56 | 21.66 | 0.000 00 | 17 | 7.16 | 0.00 030 |
| wgEncodeBroadHmmH1heschHMM_11_Weak_Txn | 61 | 47.37 | 0.00 219 | 57 | 48.33 | 0.04 144 | 26 | 19.06 | 0.01 160 | 111 | 78.53 | 0.000 00 | 39 | 31.34 | 0.03 287 |
| wgEncodeBroadHmmH1heschHMM_12_Repressed | 15 | 10.18 | 0.07 493 | 18 | 9.25 | 0.00 393 | 2 | 3.86 | 0.91 392 | 23 | 15.40 | 0.031 17 | 10 | 6.16 | 0.08 147 |
| wgEncodeBroadHmmH1heschHMM_13_Heterochrom | 86 | 87.44 | 0.76 143 | 84 | 86.36 | 0.82 505 | 29 | 32.05 | 0.96 687 | 122 | 138.45 | 0.999 97 | 53 | 57.06 | 0.95 739 |
| wgEncodeBroadHmmH1heschHMM_14_Repetitive_CNV | 1 | 0.76 | 0.53 915 | 1 | 0.68 | 0.50 187 | 0 | NA | NA | 3 | 0.96 | 0.070 81 | 0 | NA | NA |
| wgEncodeBroadHmmH1heschHMM_15_Repetitive_CNV | 1 | 0.33 | 0.28 541 | 0 | NA | NA | 0 | NA | NA | 1 | 0.44 | 0.361 35 | 0 | NA | NA |
| wgEncodeBroadHmmH1heschHMM_1_Active_Promoter | 12 | 8.67 | 0.13 989 | 15 | 7.29 | 0.00 325 | 5 | 3.35 | 0.22 573 | 25 | 12.95 | 0.000 49 | 8 | 4.19 | 0.04 640 |
| wgEncodeBroadHmmH1heschHMM_2_Weak_Promoter | 22 | 12.16 | 0.00 188 | 14 | 10.99 | 0.18 914 | 8 | 4.58 | 0.06 857 | 31 | 19.14 | 0.002 41 | 11 | 6.95 | 0.06 412 |
| wgEncodeBroadHmmH1heschHMM_3_Poised_Promoter | 13 | 6.27 | 0.00 872 | 14 | 6.48 | 0.00 432 | 3 | 2.45 | 0.44 976 | 21 | 10.27 | 0.001 15 | 5 | 4.03 | 0.37 698 |
| wgEncodeBroadHmmH1heschHMM_4_Strong_Enhancer | 3 | 2.10 | 0.35 106 | 4 | 2.00 | 0.13 373 | 0 | NA | NA | 10 | 3.11 | 0.000 97 | 1 | 0.97 | 0.63 007 |
| wgEncodeBroadHmmH1heschHMM_5_Strong_Enhancer | 2 | 4.84 | 0.96 092 | 7 | 4.69 | 0.18 308 | 3 | 1.62 | 0.21 815 | 13 | 8.19 | 0.062 05 | 7 | 2.97 | 0.02 528 |
| wgEncodeBroadHmmH1heschHMM_6_Weak_Enhancer | 31 | 22.84 | 0.02 398 | 27 | 20.73 | 0.06 259 | 12 | 8.80 | 0.12 540 | 50 | 35.51 | 0.002 25 | 11 | 12.46 | 0.73 793 |
| wgEncodeBroadHmmH1heschHMM_7_Weak_Enhancer | 35 | 31.06 | 0.20 953 | 33 | 29.29 | 0.22 132 | 19 | 12.29 | 0.01 116 | 62 | 47.85 | 0.005 96 | 24 | 19.00 | 0.09 911 |
| wgEncodeBroadHmmH1heschHMM_8_Insulator | 21 | 19.51 | 0.38 530 | 17 | 16.85 | 0.52 991 | 8 | 7.26 | 0.44 264 | 37 | 29.15 | 0.053 10 | 12 | 10.67 | 0.37 223 |
| wgEncodeBroadHmmH1heschHMM_9_Txn_Transition | 13 | 6.98 | 0.01 772 | 11 | 6.55 | 0.05 705 | 4 | 2.56 | 0.24 846 | 37 | 11.58 | 0.000 00 | 11 | 4.21 | 0.00 200 |

Enrichment of GWAS variants in epigenomic features

| | | | | | | | | | | | | | | | |
|--|----|-------|-------------|----|-------|-------------|----|-------|-------------|-----|--------|-------------|----|-------|-------------|
| wgEncodeBroadHmmHe pg2HMM_10_Txn_Elongation | 31 | 17.48 | 0.00 026 | 27 | 16.55 | 0.00 367 | 16 | 7.41 | 0.00 050 | 70 | 28.85 | 0.000 00 | 23 | 10.23 | 0.00 004 |
| wgEncodeBroadHmmHe pg2HMM_11_Weak_Txn | 44 | 33.06 | 0.00 980 | 42 | 32.94 | 0.02 928 | 20 | 13.55 | 0.01 699 | 110 | 55.50 | 0.000 00 | 32 | 20.90 | 0.00 229 |
| wgEncodeBroadHmmHe pg2HMM_12_Repressed | 28 | 19.29 | 0.01 999 | 29 | 20.15 | 0.02 045 | 13 | 8.44 | 0.05 695 | 33 | 32.12 | 0.461 83 | 13 | 12.75 | 0.51 995 |
| wgEncodeBroadHmmHe pg2HMM_13_Heterochrom | 80 | 86.10 | 0.98 158 | 85 | 84.57 | 0.52 213 | 26 | 31.65 | 0.99 803 | 103 | 136.22 | 1.000 00 | 51 | 56.02 | 0.97 414 |
| wgEncodeBroadHmmHe pg2HMM_14_Repetitive_CNV | 1 | 1.22 | 0.71 411 | 1 | 1.22 | 0.72 606 | 0 | NA | NA | 4 | 1.69 | 0.086 70 | 0 | NA | NA |
| wgEncodeBroadHmmHe pg2HMM_15_Repetitive_CNV | 3 | 1.32 | 0.14 164 | 0 | NA | NA | 0 | NA | NA | 2 | 1.68 | 0.504 58 | 1 | 0.37 | 0.31 435 |
| wgEncodeBroadHmmHe pg2HMM_1_Active_Pro_moter | 17 | 12.11 | 0.07 628 | 22 | 10.50 | 0.00 021 | 7 | 4.67 | 0.16 063 | 48 | 18.82 | 0.000 00 | 12 | 6.11 | 0.01 232 |
| wgEncodeBroadHmmHe pg2HMM_2_Weak_Pro_moter | 27 | 15.46 | 0.00 103 | 25 | 14.20 | 0.00 158 | 9 | 5.99 | 0.11 888 | 51 | 24.73 | 0.000 00 | 13 | 8.51 | 0.06 660 |
| wgEncodeBroadHmmHe pg2HMM_3_Poised_Pro_moter | 9 | 2.92 | 0.00 238 | 7 | 2.66 | 0.01 681 | 0 | NA | NA | 9 | 4.65 | 0.042 63 | 3 | 1.76 | 0.25 667 |
| wgEncodeBroadHmmHe pg2HMM_4_Strong_Enhancer | 13 | 8.58 | 0.07 815 | 10 | 7.82 | 0.25 040 | 6 | 3.10 | 0.08 079 | 52 | 13.92 | 0.000 00 | 13 | 5.01 | 0.00 092 |
| wgEncodeBroadHmmHe pg2HMM_5_Strong_Enhancer | 14 | 9.16 | 0.06 308 | 13 | 7.67 | 0.03 691 | 8 | 3.85 | 0.02 441 | 46 | 13.37 | 0.000 00 | 15 | 4.84 | 0.00 003 |
| wgEncodeBroadHmmHe pg2HMM_6_Weak_Enhancer | 33 | 22.02 | 0.00 364 | 25 | 19.73 | 0.09 967 | 12 | 8.29 | 0.08 947 | 58 | 34.87 | 0.000 00 | 26 | 12.42 | 0.00 003 |
| wgEncodeBroadHmmHe pg2HMM_7_Weak_Enhancer | 21 | 17.29 | 0.18 249 | 18 | 16.22 | 0.34 943 | 17 | 7.20 | 0.00 009 | 63 | 28.14 | 0.000 00 | 18 | 9.58 | 0.00 384 |
| wgEncodeBroadHmmHe pg2HMM_8_Insulator | 13 | 11.32 | 0.33 648 | 12 | 9.83 | 0.26 880 | 4 | 4.16 | 0.62 164 | 16 | 17.34 | 0.684 30 | 4 | 5.78 | 0.85 090 |
| wgEncodeBroadHmmHe pg2HMM_9_Txn_Transition | 17 | 10.05 | 0.01 545 | 17 | 9.05 | 0.00 574 | 7 | 3.88 | 0.07 657 | 40 | 15.81 | 0.000 00 | 14 | 5.37 | 0.00 047 |
| wgEncodeBroadHmmH mechHMM_10_Txn_Elongation | 25 | 15.37 | 0.00 515 | 28 | 15.10 | 0.00 032 | 13 | 6.36 | 0.00 440 | 65 | 26.64 | 0.000 00 | 19 | 8.96 | 0.00 054 |
| wgEncodeBroadHmmH mechHMM_11_Weak_Txn | 54 | 40.56 | 0.00 237 | 56 | 40.89 | 0.00 091 | 23 | 16.63 | 0.01 961 | 97 | 66.27 | 0.000 00 | 37 | 26.09 | 0.00 353 |

Enrichment of GWAS variants in epigenomic features

| | | | | | | | | | | | | | | | |
|--|----|-------|-------------|----|-------|-------------|----|-------|-------------|-----|--------|-------------|----|-------|-------------|
| wgEncodeBroadHmmH_mecHMM_12_Repressed | 17 | 13.75 | 0.20 275 | 20 | 13.29 | 0.03 616 | 4 | 5.49 | 0.82 447 | 23 | 20.93 | 0.344 58 | 12 | 8.41 | 0.12 522 |
| wgEncodeBroadHmmH_mecHMM_13_Heterochrom | 87 | 88.97 | 0.82 918 | 87 | 87.80 | 0.68 270 | 27 | 32.57 | 0.99 888 | 126 | 140.80 | 0.999 92 | 56 | 58.34 | 0.88 127 |
| wgEncodeBroadHmmH_mecHMM_14_Repetitive_CNV | 1 | 0.73 | 0.52 615 | 0 | NA | NA | 0 | NA | NA | 3 | 1.12 | 0.098 98 | 0 | NA | NA |
| wgEncodeBroadHmmH_mecHMM_15_Repetitive_CNV | 2 | 0.71 | 0.15 597 | 0 | NA | NA | 0 | NA | NA | 1 | 1.05 | 0.662 51 | 0 | NA | NA |
| wgEncodeBroadHmmH_mecHMM_1_Active_Promoter | 15 | 11.46 | 0.14 897 | 16 | 9.70 | 0.02 168 | 8 | 4.34 | 0.04 599 | 36 | 17.18 | 0.000 00 | 9 | 5.60 | 0.08 990 |
| wgEncodeBroadHmmH_mecHMM_2_Weak_Promoter | 16 | 9.40 | 0.01 714 | 15 | 8.45 | 0.01 533 | 5 | 3.64 | 0.28 790 | 29 | 15.35 | 0.000 25 | 9 | 4.80 | 0.04 100 |
| wgEncodeBroadHmmH_mecHMM_3_Poised_Promoter | 6 | 1.72 | 0.00 726 | 4 | 1.87 | 0.11 643 | 1 | 0.66 | 0.48 777 | 5 | 2.70 | 0.132 36 | 4 | 1.26 | 0.03 566 |
| wgEncodeBroadHmmH_mecHMM_4_Strong_Enhancer | 17 | 8.74 | 0.00 376 | 16 | 8.54 | 0.00 780 | 9 | 2.98 | 0.00 166 | 32 | 14.52 | 0.000 01 | 7 | 4.91 | 0.20 969 |
| wgEncodeBroadHmmH_mecHMM_5_Strong_Enhancer | 33 | 19.65 | 0.00 052 | 28 | 18.55 | 0.00 953 | 10 | 7.89 | 0.24 007 | 44 | 30.10 | 0.002 92 | 17 | 11.44 | 0.04 839 |
| wgEncodeBroadHmmH_mecHMM_6_Weak_Enhancer | 31 | 19.25 | 0.00 151 | 28 | 17.10 | 0.00 219 | 9 | 7.29 | 0.28 634 | 39 | 29.48 | 0.025 16 | 19 | 10.63 | 0.00 441 |
| wgEncodeBroadHmmH_mecHMM_7_Weak_Enhancer | 43 | 31.94 | 0.00 744 | 40 | 30.41 | 0.01 797 | 14 | 12.49 | 0.34 892 | 66 | 48.85 | 0.001 16 | 27 | 19.23 | 0.01 963 |
| wgEncodeBroadHmmH_mecHMM_8_Insulator | 16 | 12.11 | 0.13 542 | 14 | 10.26 | 0.13 111 | 5 | 4.50 | 0.47 810 | 26 | 17.67 | 0.020 93 | 5 | 6.30 | 0.77 984 |
| wgEncodeBroadHmmH_mecHMM_9_Txn_Transition | 7 | 5.27 | 0.27 209 | 8 | 5.04 | 0.12 514 | 4 | 1.99 | 0.13 150 | 32 | 9.24 | 0.000 00 | 5 | 3.17 | 0.20 103 |
| wgEncodeBroadHmmHs_mmHMM_10_Txn_Elongation | 38 | 20.79 | 0.00 001 | 30 | 20.08 | 0.00 805 | 20 | 8.51 | 0.00 001 | 74 | 34.36 | 0.000 00 | 24 | 12.10 | 0.00 023 |
| wgEncodeBroadHmmHs_mmHMM_11_Weak_Txn | 52 | 41.91 | 0.01 883 | 57 | 41.37 | 0.00 066 | 23 | 16.98 | 0.02 663 | 97 | 67.66 | 0.000 00 | 38 | 26.65 | 0.00 253 |
| wgEncodeBroadHmmHs_mmHMM_12_Repressed | 23 | 18.60 | 0.15 206 | 31 | 19.88 | 0.00 467 | 9 | 8.32 | 0.45 763 | 44 | 31.29 | 0.007 84 | 15 | 12.22 | 0.22 691 |
| wgEncodeBroadHmmHs_mmHMM_13_Heterochrom | 81 | 84.61 | 0.89 963 | 82 | 83.24 | 0.70 214 | 28 | 30.87 | 0.94 424 | 117 | 133.22 | 0.999 85 | 50 | 54.76 | 0.96 265 |

Enrichment of GWAS variants in epigenomic features

| | | | | | | | | | | | | | | | |
|---|----|-------|-------------|----|-------|-------------|----|-------|-------------|-----|--------|-------------|----|-------|-------------|
| wgEncodeBroadHmmHs_mmHMM_14_Repetitive_CNV | 1 | 1.33 | 0.74 407 | 0 | NA | NA | 0 | NA | NA | 5 | 2.01 | 0.048 90 | 1 | 0.73 | 0.52 509 |
| wgEncodeBroadHmmHs_mmHMM_15_Repetitive_CNV | 3 | 1.16 | 0.10 728 | 1 | 1.07 | 0.67 791 | 0 | NA | NA | 2 | 1.57 | 0.471 21 | 0 | NA | NA |
| wgEncodeBroadHmmHs_mmHMM_1_Active_Pro_moter | 16 | 10.99 | 0.06 349 | 18 | 9.34 | 0.00 275 | 5 | 3.87 | 0.34 124 | 33 | 16.71 | 0.000 03 | 10 | 5.27 | 0.02 772 |
| wgEncodeBroadHmmHs_mmHMM_2_Weak_Pro_moter | 18 | 10.80 | 0.01 362 | 15 | 9.93 | 0.05 604 | 7 | 4.28 | 0.11 280 | 37 | 17.50 | 0.000 00 | 11 | 5.86 | 0.02 297 |
| wgEncodeBroadHmmHs_mmHMM_3_Poised_Pro_moter | 10 | 2.25 | 0.00 007 | 6 | 2.32 | 0.02 798 | 0 | NA | NA | 4 | 3.55 | 0.475 96 | 3 | 1.30 | 0.13 899 |
| wgEncodeBroadHmmHs_mmHMM_4_Strong_Enhancer | 15 | 10.79 | 0.10 795 | 19 | 9.77 | 0.00 265 | 9 | 3.99 | 0.01 264 | 33 | 15.66 | 0.000 02 | 9 | 6.26 | 0.16 228 |
| wgEncodeBroadHmmHs_mmHMM_5_Strong_Enhancer | 27 | 18.37 | 0.01 576 | 26 | 16.43 | 0.00 728 | 10 | 7.26 | 0.16 368 | 47 | 26.82 | 0.000 02 | 14 | 10.46 | 0.14 401 |
| wgEncodeBroadHmmHs_mmHMM_6_Weak_Enhancer | 35 | 20.34 | 0.00 014 | 28 | 18.82 | 0.00 996 | 13 | 7.55 | 0.01 812 | 49 | 30.26 | 0.000 08 | 16 | 11.07 | 0.06 567 |
| wgEncodeBroadHmmHs_mmHMM_7_Weak_Enhancer | 31 | 24.42 | 0.06 768 | 38 | 22.82 | 0.00 019 | 15 | 9.86 | 0.03 500 | 51 | 36.97 | 0.004 45 | 22 | 14.00 | 0.01 203 |
| wgEncodeBroadHmmHs_mmHMM_8_Insulator | 17 | 14.13 | 0.22 879 | 15 | 12.35 | 0.23 772 | 8 | 5.51 | 0.15 601 | 25 | 20.92 | 0.182 80 | 7 | 7.21 | 0.59 872 |
| wgEncodeBroadHmmHs_mmHMM_9_Txn_Transition | 17 | 9.97 | 0.01 494 | 15 | 9.74 | 0.05 134 | 10 | 3.66 | 0.00 167 | 43 | 16.67 | 0.000 00 | 12 | 5.55 | 0.00 647 |
| wgEncodeBroadHmmHu_vecHMM_10_Txn_Elongation | 25 | 14.96 | 0.00 350 | 26 | 14.20 | 0.00 068 | 14 | 6.00 | 0.00 070 | 58 | 24.51 | 0.000 00 | 19 | 8.29 | 0.00 019 |
| wgEncodeBroadHmmHu_vecHMM_11_Weak_Txn | 44 | 34.74 | 0.02 386 | 47 | 33.96 | 0.00 300 | 19 | 13.82 | 0.04 670 | 91 | 56.69 | 0.000 00 | 35 | 21.63 | 0.00 034 |
| wgEncodeBroadHmmHu_vecHMM_12_Repressed | 32 | 27.03 | 0.14 665 | 28 | 27.98 | 0.53 792 | 16 | 11.49 | 0.07 308 | 60 | 44.52 | 0.003 71 | 21 | 17.04 | 0.15 885 |
| wgEncodeBroadHmmHu_vecHMM_13_Heterochrom | 81 | 88.01 | 0.99 411 | 84 | 87.05 | 0.87 748 | 29 | 32.35 | 0.97 855 | 127 | 139.56 | 0.999 28 | 54 | 57.58 | 0.94 331 |
| wgEncodeBroadHmmHu_vecHMM_14_Repetitive_CNV | 1 | 1.56 | 0.79 910 | 1 | 1.40 | 0.76 423 | 1 | 0.59 | 0.46 005 | 6 | 2.34 | 0.028 66 | 0 | NA | NA |
| wgEncodeBroadHmmHu_vecHMM_15_Repetitive_CNV | 5 | 1.78 | 0.02 991 | 1 | 1.55 | 0.81 037 | 0 | NA | NA | 3 | 2.09 | 0.348 83 | 1 | 0.54 | 0.42 469 |
| wgEncodeBroadHmmHu_vecHMM_1_Active_Pro | 16 | 10.10 | 0.03 150 | 15 | 8.71 | 0.01 838 | 6 | 3.97 | 0.18 168 | 33 | 15.29 | 0.000 00 | 7 | 4.98 | 0.21 588 |

Enrichment of GWAS variants in epigenomic features

| moter | | | | | | | | | | | | | | | |
|--|----|-------|-------------|----|-------|-------------|----|-------|-------------|-----|--------|-------------|----|-------|-------------|
| wgEncodeBroadHmmHu vecHMM_2_Weak_Pro moter | 19 | 8.98 | 0.00 057 | 12 | 8.48 | 0.12 478 | 6 | 3.41 | 0.10 522 | 27 | 14.19 | 0.000 40 | 4 | 4.28 | 0.63 828 |
| wgEncodeBroadHmmHu vecHMM_3_Poised_Pro moter | 5 | 2.86 | 0.15 532 | 5 | 3.31 | 0.23 304 | 2 | 1.01 | 0.26 776 | 6 | 4.68 | 0.326 08 | 4 | 1.72 | 0.08 893 |
| wgEncodeBroadHmmHu vecHMM_4_Strong_Enh ancer | 21 | 13.44 | 0.01 763 | 27 | 12.01 | 0.00 001 | 9 | 4.75 | 0.03 485 | 34 | 19.98 | 0.000 72 | 17 | 7.23 | 0.00 034 |
| wgEncodeBroadHmmHu vecHMM_5_Strong_Enh ancer | 27 | 16.59 | 0.00 357 | 30 | 15.47 | 0.00 008 | 10 | 6.48 | 0.08 862 | 45 | 25.01 | 0.000 02 | 14 | 9.21 | 0.06 286 |
| wgEncodeBroadHmmHu vecHMM_6_Weak_Enha ncer | 11 | 13.60 | 0.83 641 | 22 | 11.74 | 0.00 135 | 3 | 5.05 | 0.91 056 | 35 | 20.80 | 0.000 53 | 8 | 6.89 | 0.38 235 |
| wgEncodeBroadHmmHu vecHMM_7_Weak_Enha ncer | 24 | 23.87 | 0.53 160 | 37 | 22.37 | 0.00 026 | 12 | 9.42 | 0.19 680 | 57 | 36.74 | 0.000 05 | 23 | 13.53 | 0.00 307 |
| wgEncodeBroadHmmHu vecHMM_8_Insulator | 17 | 13.51 | 0.17 302 | 15 | 11.20 | 0.13 812 | 5 | 4.94 | 0.57 024 | 30 | 19.98 | 0.009 99 | 7 | 6.72 | 0.51 725 |
| wgEncodeBroadHmmHu vecHMM_9_Txn_Transit ion | 10 | 7.65 | 0.22 563 | 13 | 6.47 | 0.00 959 | 5 | 2.31 | 0.07 353 | 34 | 11.31 | 0.000 00 | 10 | 4.01 | 0.00 468 |
| wgEncodeBroadHmmK5 62HMM_10_Txn_Elonga tion | 26 | 15.40 | 0.00 224 | 26 | 14.13 | 0.00 061 | 12 | 6.38 | 0.01 160 | 58 | 25.28 | 0.000 00 | 16 | 8.50 | 0.00 622 |
| wgEncodeBroadHmmK5 62HMM_11_Weak_Txn | 52 | 33.39 | 0.00 003 | 42 | 33.56 | 0.03 989 | 15 | 13.59 | 0.36 731 | 107 | 54.79 | 0.000 00 | 27 | 20.96 | 0.06 649 |
| wgEncodeBroadHmmK5 62HMM_12_Repressed | 26 | 26.00 | 0.53 977 | 38 | 28.61 | 0.02 441 | 16 | 10.95 | 0.05 172 | 55 | 44.15 | 0.032 39 | 26 | 17.76 | 0.01 658 |
| wgEncodeBroadHmmK5 62HMM_13_Heterochro m | 79 | 83.70 | 0.94 054 | 72 | 82.03 | 0.99 751 | 26 | 30.71 | 0.99 057 | 108 | 131.89 | 1.000 00 | 53 | 54.46 | 0.75 957 |
| wgEncodeBroadHmmK5 62HMM_14_Repetitive_ CNV | 2 | 2.05 | 0.61 663 | 0 | NA | NA | 0 | NA | NA | 6 | 2.88 | 0.067 86 | 1 | 1.07 | 0.66 296 |
| wgEncodeBroadHmmK5 62HMM_15_Repetitive_ CNV | 4 | 1.96 | 0.12 842 | 2 | 1.76 | 0.53 543 | 0 | NA | NA | 4 | 2.79 | 0.304 97 | 2 | 0.83 | 0.20 096 |
| wgEncodeBroadHmmK5 62HMM_1_Active_Prom oter | 19 | 12.11 | 0.02 035 | 19 | 10.35 | 0.00 354 | 6 | 4.66 | 0.31 026 | 43 | 18.56 | 0.000 00 | 8 | 5.78 | 0.20 960 |
| wgEncodeBroadHmmK5 62HMM_2_Weak_Prom oter | 17 | 11.26 | 0.04 152 | 15 | 10.55 | 0.08 612 | 5 | 4.41 | 0.45 733 | 33 | 17.20 | 0.000 06 | 7 | 5.79 | 0.35 585 |
| wgEncodeBroadHmmK5 62HMM_3_Poised_Pro moter | 3 | 2.19 | 0.37 468 | 7 | 2.60 | 0.01 347 | 1 | 0.96 | 0.62 752 | 7 | 4.08 | 0.112 76 | 1 | 1.49 | 0.78 653 |

Enrichment of GWAS variants in epigenomic features

| | | | | | | | | | | | | | | | |
|--|----|-------|-------------|----|-------|-------------|----|-------|-------------|-----|--------|-------------|----|-------|-------------|
| wgEncodeBroadHmmK5_62HMM_4_Strong_Enhancer | 18 | 11.15 | 0.02 121 | 20 | 10.26 | 0.00 178 | 7 | 4.55 | 0.15 212 | 40 | 18.03 | 0.000 00 | 9 | 6.45 | 0.18 388 |
| wgEncodeBroadHmmK5_62HMM_5_Strong_Enhancer | 17 | 10.50 | 0.02 439 | 17 | 9.37 | 0.00 885 | 8 | 4.35 | 0.04 963 | 42 | 16.31 | 0.000 00 | 9 | 5.83 | 0.11 565 |
| wgEncodeBroadHmmK5_62HMM_6_Weak_Enhancer | 20 | 16.29 | 0.16 977 | 20 | 13.71 | 0.03 982 | 6 | 5.93 | 0.56 655 | 25 | 24.89 | 0.528 97 | 9 | 8.31 | 0.45 355 |
| wgEncodeBroadHmmK5_62HMM_7_Weak_Enhancer | 30 | 25.19 | 0.14 159 | 33 | 24.27 | 0.02 225 | 11 | 10.06 | 0.42 168 | 75 | 39.17 | 0.000 00 | 19 | 14.35 | 0.09 998 |
| wgEncodeBroadHmmK5_62HMM_8_Insulator | 17 | 15.63 | 0.38 943 | 18 | 14.00 | 0.14 298 | 6 | 5.92 | 0.56 352 | 38 | 23.67 | 0.000 89 | 13 | 8.04 | 0.04 696 |
| wgEncodeBroadHmmK5_62HMM_9_Txn_Transition | 20 | 10.49 | 0.00 197 | 22 | 9.36 | 0.00 005 | 14 | 4.13 | 0.00 001 | 41 | 16.57 | 0.000 00 | 10 | 6.01 | 0.06 522 |
| wgEncodeBroadHmmNh_ekHMM_10_Txn_Elongation | 30 | 16.53 | 0.00 026 | 28 | 16.40 | 0.00 140 | 15 | 6.69 | 0.00 071 | 71 | 28.48 | 0.000 00 | 21 | 9.99 | 0.00 028 |
| wgEncodeBroadHmmNh_ekHMM_11_Weak_Txn | 46 | 37.85 | 0.04 543 | 48 | 38.08 | 0.02 125 | 18 | 15.56 | 0.24 564 | 100 | 62.14 | 0.000 00 | 35 | 24.18 | 0.00 343 |
| wgEncodeBroadHmmNh_ekHMM_12_Repressed | 29 | 21.79 | 0.05 078 | 32 | 22.05 | 0.01 260 | 16 | 8.96 | 0.00 741 | 45 | 34.85 | 0.032 43 | 19 | 13.97 | 0.08 596 |
| wgEncodeBroadHmmNh_ekHMM_13_Heterochrom | 85 | 87.43 | 0.85 045 | 83 | 85.47 | 0.82 461 | 25 | 31.95 | 0.99 977 | 122 | 137.75 | 0.999 92 | 52 | 56.68 | 0.97 122 |
| wgEncodeBroadHmmNh_ekHMM_14_Repetitive_CNV | 0 | NA | NA | 1 | 0.77 | 0.54 697 | 1 | 0.30 | 0.26 567 | 2 | 0.99 | 0.259 08 | 0 | NA | NA |
| wgEncodeBroadHmmNh_ekHMM_15_Repetitive_CNV | 1 | 0.34 | 0.29 347 | 0 | NA | NA | 0 | NA | NA | 1 | 0.45 | 0.372 21 | 0 | NA | NA |
| wgEncodeBroadHmmNh_ekHMM_1_Active_Promoter | 17 | 11.84 | 0.06 250 | 17 | 10.56 | 0.02 250 | 7 | 4.60 | 0.14 893 | 36 | 18.45 | 0.000 01 | 10 | 6.12 | 0.06 757 |
| wgEncodeBroadHmmNh_ekHMM_2_Weak_Promoter | 13 | 8.95 | 0.09 668 | 17 | 8.29 | 0.00 195 | 7 | 3.62 | 0.05 276 | 31 | 13.58 | 0.000 00 | 5 | 4.37 | 0.44 708 |
| wgEncodeBroadHmmNh_ekHMM_3_Poised_Promoter | 5 | 3.39 | 0.25 070 | 4 | 3.22 | 0.40 325 | 2 | 1.31 | 0.37 839 | 7 | 5.22 | 0.265 65 | 4 | 2.25 | 0.17 985 |
| wgEncodeBroadHmmNh_ekHMM_4_Strong_Enhancer | 28 | 12.41 | 0.00 001 | 16 | 11.88 | 0.12 154 | 11 | 4.62 | 0.00 323 | 37 | 19.42 | 0.000 03 | 11 | 7.33 | 0.10 129 |
| wgEncodeBroadHmmNh_ekHMM_5_Strong_Enhancer | 30 | 17.51 | 0.00 075 | 30 | 16.78 | 0.00 037 | 8 | 7.34 | 0.45 680 | 46 | 26.86 | 0.000 04 | 14 | 9.91 | 0.10 164 |
| wgEncodeBroadHmmNh_ekHMM_6_Weak_Enhancer | 24 | 18.30 | 0.07 473 | 27 | 16.01 | 0.00 186 | 2 | 6.74 | 0.99 652 | 38 | 27.52 | 0.014 15 | 18 | 9.83 | 0.00 449 |

Enrichment of GWAS variants in epigenomic features

| ncer | | | | | | | | | | | | | | | |
|--|----|-------|-------------|----|-------|-------------|----|-------|-------------|-----|--------|-------------|----|-------|-------------|
| wgEncodeBroadHmmNh_ekHMM_7_Weak_Enhancer | 35 | 28.09 | 0.06 011 | 35 | 25.93 | 0.01 945 | 14 | 10.44 | 0.11 779 | 64 | 42.15 | 0.000 03 | 23 | 15.96 | 0.02 605 |
| wgEncodeBroadHmmNh_ekHMM_8_Insulator | 20 | 16.38 | 0.18 127 | 15 | 14.11 | 0.44 136 | 6 | 6.03 | 0.58 342 | 36 | 24.78 | 0.007 39 | 9 | 8.82 | 0.53 272 |
| wgEncodeBroadHmmNh_ekHMM_9_Txn_Transition | 12 | 6.95 | 0.03 933 | 10 | 6.37 | 0.09 830 | 4 | 2.64 | 0.26 818 | 31 | 11.47 | 0.000 00 | 5 | 4.16 | 0.40 400 |
| wgEncodeBroadHmmNh_lfHMM_10_Txn_Elongation | 29 | 16.83 | 0.00 086 | 27 | 16.16 | 0.00 256 | 17 | 6.89 | 0.00 006 | 68 | 28.36 | 0.000 00 | 21 | 9.83 | 0.00 024 |
| wgEncodeBroadHmmNh_lfHMM_11_Weak_Txn | 47 | 37.41 | 0.02 239 | 55 | 36.94 | 0.00 008 | 24 | 15.43 | 0.00 223 | 97 | 60.85 | 0.000 00 | 37 | 24.21 | 0.00 062 |
| wgEncodeBroadHmmNh_lfHMM_12_Repressed | 31 | 25.33 | 0.10 947 | 36 | 26.77 | 0.02 373 | 11 | 10.55 | 0.49 792 | 62 | 41.58 | 0.000 19 | 28 | 16.72 | 0.00 143 |
| wgEncodeBroadHmmNh_lfHMM_13_Heterochrom | 83 | 86.70 | 0.92 119 | 83 | 85.70 | 0.84 432 | 27 | 31.72 | 0.99 412 | 120 | 137.01 | 0.999 97 | 54 | 56.38 | 0.86 236 |
| wgEncodeBroadHmmNh_lfHMM_14_Repetitive_CNV | 0 | NA | NA | 0 | NA | NA | 1 | 0.17 | 0.15 724 | 4 | 0.97 | 0.014 67 | 1 | 0.38 | 0.32 084 |
| wgEncodeBroadHmmNh_lfHMM_15_Repetitive_CNV | 4 | 1.69 | 0.08 382 | 1 | 1.36 | 0.76 471 | 0 | NA | NA | 2 | 2.01 | 0.605 03 | 1 | 0.57 | 0.44 501 |
| wgEncodeBroadHmmNh_lfHMM_1_Active_Promoter | 20 | 11.78 | 0.00 699 | 23 | 10.36 | 0.00 006 | 7 | 4.61 | 0.15 176 | 37 | 18.13 | 0.000 00 | 12 | 5.94 | 0.00 898 |
| wgEncodeBroadHmmNh_lfHMM_2_Weak_Promoter | 18 | 10.52 | 0.01 013 | 16 | 9.43 | 0.01 845 | 6 | 4.07 | 0.20 421 | 30 | 16.88 | 0.000 63 | 5 | 5.45 | 0.65 508 |
| wgEncodeBroadHmmNh_lfHMM_3_Poised_Promoter | 5 | 2.07 | 0.05 610 | 3 | 2.12 | 0.35 538 | 0 | NA | NA | 5 | 3.92 | 0.355 24 | 1 | 1.30 | 0.73 465 |
| wgEncodeBroadHmmNh_lfHMM_4_Strong_Enhancer | 9 | 5.56 | 0.09 768 | 17 | 5.12 | 0.00 001 | 5 | 2.33 | 0.07 356 | 21 | 8.75 | 0.000 12 | 6 | 3.21 | 0.09 473 |
| wgEncodeBroadHmmNh_lfHMM_5_Strong_Enhancer | 24 | 15.17 | 0.01 013 | 28 | 13.86 | 0.00 009 | 7 | 5.92 | 0.37 745 | 41 | 22.68 | 0.000 05 | 16 | 8.35 | 0.00 575 |
| wgEncodeBroadHmmNh_lfHMM_6_Weak_Enhancer | 27 | 16.73 | 0.00 351 | 23 | 15.55 | 0.02 289 | 8 | 6.82 | 0.36 214 | 38 | 26.11 | 0.005 64 | 16 | 9.12 | 0.01 123 |
| wgEncodeBroadHmmNh_lfHMM_7_Weak_Enhancer | 38 | 24.18 | 0.00 065 | 34 | 22.99 | 0.00 485 | 15 | 9.66 | 0.02 947 | 66 | 37.50 | 0.000 00 | 23 | 14.12 | 0.00 594 |
| wgEncodeBroadHmmNh_lfHMM_8_Insulator | 25 | 20.35 | 0.13 187 | 24 | 17.83 | 0.05 945 | 10 | 7.49 | 0.18 780 | 39 | 30.63 | 0.044 94 | 13 | 10.68 | 0.25 547 |
| wgEncodeBroadHmmNh | 10 | 6.52 | 0.10 | 16 | 5.74 | 0.00 | 6 | 2.41 | 0.02 | 31 | 10.39 | 0.000 | 8 | 3.56 | 0.02 |

| | | | | | | | | | | | | | | | |
|------------------------|--|--|-----|--|--|-----|--|--|-----|--|--|----|--|--|-----|
| IfHMM_9_Txn_Transition | | | 888 | | | 010 | | | 636 | | | 00 | | | 218 |
|------------------------|--|--|-----|--|--|-----|--|--|-----|--|--|----|--|--|-----|

Supplementary Table 5. Enrichment of lipid loci in transcription factor binding sites and histone modifications from relevant Tier 1 and Tier 2 cell types.

| Feature | InBed_Index_SNP | ExpectNum_of_InBed_SNP | PValue | Annotation |
|------------|-----------------|------------------------|----------|----------------------|
| POLR2A | 116 | 59.17 | 6.23E-24 | |
| RCOR1 | 87 | 41.86 | 1.75E-16 | |
| SP1 | 52 | 17.29 | 1.48E-15 | |
| EP300 | 82 | 40.67 | 1.08E-14 | literature |
| eGFP_JUND | 86 | 43.98 | 2.20E-14 | |
| H3K4me3 | 72 | 34.27 | 1.38E-13 | literature |
| MXI1 | 62 | 26.53 | 2.79E-13 | |
| MYC | 71 | 33.76 | 5.75E-13 | |
| H3K36me3 | 52 | 20.55 | 1.07E-12 | |
| MYBL2 | 39 | 11.69 | 1.17E-12 | |
| TBL1XR1 | 63 | 29.30 | 8.89E-12 | lipid gene regulator |
| H3K9me1 | 111 | 70.65 | 2.11E-11 | literature |
| SMC3 | 63 | 30.21 | 2.57E-11 | |
| ARID3A | 68 | 34.44 | 3.44E-11 | |
| H3k4me1 | 74 | 38.57 | 4.82E-11 | |
| H3K9ac | 56 | 25.49 | 1.25E-10 | |
| MAZ | 70 | 37.11 | 3.52E-10 | |
| BHLHE40 | 67 | 34.86 | 4.42E-10 | |
| TBP | 57 | 27.07 | 4.95E-10 | |
| eGFP_GATA2 | 64 | 32.64 | 7.25E-10 | |
| MAX | 63 | 32.05 | 7.86E-10 | |
| JUND | 85 | 52.19 | 1.04E-09 | |
| NCOR1 | 81 | 45.39 | 1.22E-09 | lipid gene regulator |
| FOXA1 | 46 | 20.41 | 5.00E-09 | lipid gene regulator |

Enrichment of GWAS variants in epigenomic features

| | | | | |
|------------|----|-------|----------|----------------------|
| NFIC | 48 | 21.88 | 6.26E-09 | |
| TEAD4 | 44 | 19.11 | 7.09E-09 | |
| TAL1 | 49 | 23.02 | 1.08E-08 | |
| CEBPB | 90 | 59.99 | 1.69E-08 | lipid gene regulator |
| CCNT2 | 49 | 23.51 | 1.99E-08 | |
| HDAC2 | 33 | 12.05 | 2.13E-08 | |
| HNF4G | 26 | 7.82 | 2.19E-08 | |
| RFX5 | 48 | 23.02 | 2.20E-08 | |
| eGFP_JUNB | 52 | 25.73 | 2.39E-08 | literature |
| RXRA | 25 | 7.50 | 4.23E-08 | lipid gene regulator |
| ELF1 | 40 | 17.21 | 4.38E-08 | |
| JUN | 61 | 34.37 | 1.08E-07 | |
| CREB1 | 45 | 21.64 | 1.10E-07 | literature |
| CHD2 | 47 | 23.26 | 1.65E-07 | |
| eGFP_HDAC8 | 24 | 7.62 | 2.51E-07 | |
| HMGN3 | 43 | 20.66 | 3.08E-07 | |
| CUX1 | 40 | 18.64 | 4.04E-07 | |
| ZNF143 | 51 | 27.20 | 4.49E-07 | |
| CTCF | 75 | 49.00 | 7.41E-07 | |
| ZC3H11A | 32 | 13.68 | 1.29E-06 | |
| HNF4A | 28 | 10.93 | 1.66E-06 | lipid gene regulator |
| IRF1 | 49 | 26.87 | 1.71E-06 | |
| YY1 | 42 | 21.34 | 2.22E-06 | literature |
| TCF7L2 | 23 | 8.15 | 2.28E-06 | literature |
| USF2 | 30 | 12.76 | 2.98E-06 | |
| MBD4 | 16 | 4.26 | 3.52E-06 | |
| ZNF384 | 47 | 25.87 | 3.84E-06 | |
| SIN3AK20 | 28 | 11.66 | 3.93E-06 | |
| NFYA | 20 | 6.79 | 7.28E-06 | |
| SPI1 | 37 | 18.56 | 8.45E-06 | |
| BRCA1 | 22 | 8.21 | 9.76E-06 | |
| RAD21 | 52 | 31.14 | 1.22E-05 | |

Enrichment of GWAS variants in epigenomic features

| | | | | |
|------------|----|-------|----------|----------------------|
| SREBP1 | 11 | 2.29 | 1.40E-05 | lipid gene regulator |
| E2F6 | 35 | 17.56 | 1.48E-05 | |
| HDAC1 | 22 | 8.52 | 1.85E-05 | literature |
| ZBTB7A | 25 | 10.54 | 2.06E-05 | |
| UBTF | 32 | 15.91 | 3.31E-05 | |
| HCFC1 | 38 | 20.75 | 4.65E-05 | |
| TAF1 | 29 | 13.98 | 4.65E-05 | |
| TCF12 | 20 | 7.85 | 7.83E-05 | |
| E2F4 | 23 | 10.14 | 8.46E-05 | |
| CEBPD | 16 | 5.54 | 8.69E-05 | lipid gene regulator |
| EGR1 | 28 | 13.53 | 8.85E-05 | |
| KDM5B | 23 | 10.22 | 0.00010 | |
| PML | 32 | 17.10 | 0.00014 | |
| RUNX3 | 40 | 23.82 | 0.00021 | |
| USF1 | 26 | 12.74 | 0.00021 | lipid gene regulator |
| FOS | 15 | 5.37 | 0.00022 | |
| EBF1 | 31 | 16.38 | 0.00023 | |
| FOXA2 | 29 | 15.33 | 0.00029 | lipid gene regulator |
| eGFP_FOS | 30 | 16.04 | 0.00031 | |
| REST | 25 | 12.46 | 0.00033 | |
| FOSL2 | 20 | 8.83 | 0.00036 | |
| GTF2F1 | 24 | 11.97 | 0.00040 | |
| CHD1 | 20 | 9.14 | 0.00046 | |
| eGFP_NR4A1 | 11 | 3.50 | 0.00067 | literature |
| ATF1 | 35 | 21.01 | 0.00069 | |
| POU2F2 | 21 | 10.12 | 0.00074 | |
| SAP30 | 17 | 7.44 | 0.00078 | |
| CEBPZ | 6 | 1.17 | 0.00095 | literature |
| NR2F2 | 20 | 9.62 | 0.00101 | |
| PHF8 | 25 | 13.65 | 0.00124 | |
| MAFF | 59 | 43.42 | 0.00130 | |
| ELK1 | 20 | 10.04 | 0.00166 | |

Enrichment of GWAS variants in epigenomic features

| | | | | |
|----------|----|-------|---------|----------------------|
| MAFK | 75 | 59.30 | 0.00170 | |
| ATF3 | 16 | 7.46 | 0.00248 | literature |
| SREBP2 | 2 | 0.08 | 0.00278 | lipid gene regulator |
| GATA2 | 20 | 10.47 | 0.00284 | |
| SIN3A | 17 | 8.47 | 0.00337 | |
| GTF2B | 16 | 7.77 | 0.00338 | |
| WRNIP1 | 16 | 7.77 | 0.00360 | |
| ETS1 | 15 | 7.06 | 0.00366 | |
| SIX5 | 9 | 3.16 | 0.00380 | |
| KAP1 | 28 | 17.39 | 0.00417 | |
| IRF4 | 16 | 8.10 | 0.00570 | |
| CREBBP | 87 | 70.93 | 0.00590 | lipid gene regulator |
| ZEB1 | 8 | 2.80 | 0.00629 | |
| GTF3C2 | 7 | 2.27 | 0.00698 | |
| PAX5 | 22 | 13.06 | 0.00832 | |
| GABPA | 18 | 10.15 | 0.01012 | |
| NR2C2 | 8 | 3.08 | 0.01097 | literature |
| NFYB | 24 | 15.13 | 0.01193 | |
| STAT1 | 10 | 4.52 | 0.01362 | |
| RBBP5 | 18 | 10.59 | 0.01497 | |
| FOSL1 | 9 | 4.03 | 0.01757 | |
| GATA1 | 17 | 10.02 | 0.02008 | |
| MTA3 | 15 | 8.61 | 0.02249 | |
| SMARCA4 | 7 | 2.90 | 0.02391 | |
| NRF1 | 11 | 5.69 | 0.02427 | lipid gene regulator |
| SIRT6 | 5 | 1.67 | 0.02492 | lipid gene regulator |
| ATF2 | 20 | 12.81 | 0.02558 | literature |
| STAT2 | 7 | 2.92 | 0.02602 | |
| PBX3 | 8 | 3.77 | 0.03296 | |
| H3k27me3 | 46 | 35.95 | 0.03437 | literature |
| SP2 | 6 | 2.54 | 0.04047 | |
| ZBTB33 | 7 | 3.23 | 0.04068 | |

Enrichment of GWAS variants in epigenomic features

| | | | | |
|---------|-----|--------|---------|------------|
| NFE2 | 5 | 1.92 | 0.04189 | |
| CTCFL | 7 | 3.29 | 0.04599 | |
| BCLAF1 | 11 | 6.32 | 0.04747 | |
| RPC155 | 3 | 0.88 | 0.05834 | |
| STAT5A | 15 | 10.13 | 0.07479 | |
| STAT3 | 7 | 3.71 | 0.07701 | |
| GRp20 | 2 | 0.50 | 0.08754 | |
| THAP1 | 5 | 2.46 | 0.09661 | |
| ZNF274 | 9 | 5.55 | 0.10080 | |
| MEF2A | 13 | 8.91 | 0.10277 | |
| BACH1 | 12 | 8.42 | 0.13021 | literature |
| TAF7 | 5 | 2.74 | 0.13566 | |
| IRF3 | 2 | 0.67 | 0.14483 | literature |
| BATF | 14 | 10.35 | 0.14632 | |
| RELA | 12 | 8.71 | 0.15678 | |
| ESRRα | 2 | 0.72 | 0.15937 | |
| TCF3 | 10 | 7.04 | 0.16372 | |
| EZH2 | 5 | 3.06 | 0.19139 | literature |
| BCL3 | 10 | 7.33 | 0.19457 | |
| IKZF1 | 8 | 6.00 | 0.25050 | |
| MEF2C | 6 | 4.34 | 0.26304 | |
| SMARCB1 | 3 | 1.84 | 0.27931 | |
| TRIM28 | 10 | 8.17 | 0.29765 | literature |
| NFATC1 | 9 | 7.25 | 0.29894 | |
| HSF1 | 2 | 1.15 | 0.31948 | |
| FOXM1 | 15 | 13.35 | 0.35378 | literature |
| SETDB1 | 8 | 6.90 | 0.38417 | |
| RDBP | 1 | 0.49 | 0.39523 | |
| HDAC6 | 1 | 0.54 | 0.42744 | |
| SRF | 6 | 5.34 | 0.44601 | |
| ZNF263 | 3 | 2.73 | 0.51755 | |
| H3K9me3 | 116 | 119.25 | 0.77337 | literature |

| | | | | |
|----------|---|----|----|----------------------|
| BDP1 | 0 | NA | NA | |
| BRF1 | 0 | NA | NA | |
| POLR3G | 0 | NA | NA | |
| PPARGC1A | 0 | NA | NA | lipid gene regulator |
| XRCC4 | 0 | NA | NA | |
| ZZZ3 | 0 | NA | NA | |

Supplementary Table 6: Primers used in luciferase expression constructs.

| | | |
|---------|-------------|------------------------|
| SPTLC3 | Rs1321940F | GTGCTCACTGAAACGTGTCT |
| | Rs1321940R | CAGTGACAATGTCAATATGGA |
| | | |
| | Rs364585F | CACCTGACCATTCTCCCCA |
| | Rs364585R | ACGAAACACCCCTGAAGACA |
| | | |
| ANGPTL8 | Rs3810308F | AGAGGGAGGCAGAACGTGAAGG |
| | Rs3810308R | CCAGCTCTGAACTCTGGACA |
| | | |
| | Rs737337F | GGGTAGGGATGTGGAGTGAG |
| | Rs737337R | ATTCCCATTGCCTCTGTGCT |
| | | |
| FAM117B | Rs11692610F | TAAAAGCCCGAACGAGATGC |
| | Rs11692610R | GGGTTTGTGTTGTTGGGC |
| | | |
| | Rs11694172F | TCCTGGGTTCAAGCAGTTCT |
| | Rs11694172R | ATCCCAAAGGCCTCCAAAGA |
| | | |
| | | |
| SORT1 | Rs12740374F | ACACATTTCAGGGGAGCCT |

| | | |
|---------|-------------|------------------------|
| | Rs12740374R | AGGAGAGGTGGGGAGATGAT |
| | | |
| | Rs629301F | TCTCCTCAGTTTGCCGACT |
| | Rs629301R | CTCTCCCACCGTAGAAGTCC |
| | | |
| IRF2BP2 | Rs526936F | AAAAGTAGCTGGCGTGGTA |
| | Rs526936R | CCCCGAGTAAACACCCCTCT |
| | | |
| | Rs514230F | CCCCAGACATGAGGAACAAGT |
| | Rs514230R | GCAGGCCGGTTTCTTCTTT |
| | | |
| ADH5 | Rs2602836F | GCCAGCAATGAACAAAGTGGAA |
| | Rs2602836R | CGCACATGTAACAAACCTGC |
| | | |
| | Rs1800759F | CTGGCATAGGGGTCACTCAT |
| | Rs1800759R | AATGGGCGATTCTGAGGAGT |

SUPPLEMENTARY REFERENCES

- Boyle, A.P., et al. (2012) Annotation of functional variation in personal genomes using RegulomeDB, *Genome research*, **22**, 1790-1797.
- Ernst, J., et al. (2011) Mapping and analysis of chromatin state dynamics in nine human cell types, *Nature*, **473**, 43-49.
- Parker, S.C., et al. (2013) Chromatin stretch enhancer states drive cell-specific gene regulation and harbor human disease risk variants, *Proceedings of the National Academy of Sciences of the United States of America*, **110**, 17921-17926.
- Te Grotenhuis, M., Eisinga, R. and Pelzer, B. (2013) Saddlepoint approximations for the sum of independent non-identically distributed binomial random variables, *Statistica Neerlandica*, **67**, 190-201.
- Teslovich, T.M., et al. (2010) Biological, clinical and population relevance of 95 loci for blood lipids, *Nature*, **466**, 707-713.
- The ENCODE Project Consortium (2012) An integrated encyclopedia of DNA elements in the human genome, *Nature*, **489**, 57-74.
- Willer, C.J., et al. (2013) Discovery and refinement of loci associated with lipid levels, *Nat Genet*, **45**, 1274-1283.